

THE PRODUCTION OF VACANCIES DURING REVERSED PLASTIC FLOW

THE PRODUCTION OF VACANCIES DURING REVERSED PLASTIC FLOW

by

DONALD JAFFREY B.Sc.

A Thesis

Submitted to the Faculty of Graduate Studies

in Partial Fulfilment of the Requirements

for the Degree

Master of Science

McMaster University

May 1966

MASTER OF SCIENCE (1966)
(Metallurgy)

McMASTER UNIVERSITY
Hamilton, Ontario

TITLE: The Production of Vacancies During Reversed Plastic Flow

AUTHOR: Donald Jaffrey B.Sc. (Honours) University of Queensland

SUPERVISOR: Associate Professor R. K. Ham

NUMBER OF PAGES: vii, 62

CONTENTS: The Portevin-le Chatelier effect in a copper-3.2 at.% tin alloy has been used to investigate the rate of vacancy production during reversed plastic flow. The production rate per unit strain has been shown to be approximately half the value found for straight tensile deformation. It was inferred from this that fatigue is not a highly efficient method for producing vacancies.

The relationship between the dislocation density and the tensile plastic strain for this alloy has been determined by transmission electron microscopy. It was found to obey the law,

$$\rho = \text{const. } \epsilon^{1.17 \pm 0.13}$$

It was also found that during reversed plastic flow this law was no longer valid.

ACKNOWLEDGEMENTS

The author is deeply indebted to Dr. R. K. Ham for his supervision, assistance and encouragement throughout the duration of this work and during the preparation of this thesis.

The material was supplied by Dr. B. Russell, University of Queensland, Brisbane, Australia, and this is gratefully acknowledged.

The author also wishes to thank McMaster University for the provision of a scholarship and the National Research Council for financial support.

TABLE OF CONTENTS

Section	Subject	Page
1	Introduction	1
2	Review of Previous Work	4
2.1	Production of Vacancies	4
2.1.1	Production of Vacancy Loops by Quenching, Irradiation and Unidirectional Deformation	4
2.1.2	Theory of Vacancy Production During Fatigue	7
2.1.3	Evidence of Vacancy Production from Trans- mission Electron Microscopy	9
2.1.4	Other Evidence	13
2.2	The Portevin-le Chatelier Effect	16
2.2.1	General Discussion	16
2.2.2	The P-L Effect in Cu-Sn Primary Solid Solutions	23
2.3	Dislocation Density as a Function of Stress or Strain	26
2.4	Annihilation of Dislocations During Reversed Plastic Flow	30
3	Experimental Details	33
3.1	Materials and Specimen Preparation	33
3.2	Equipment	35
3.3	Experimental Techniques	36
3.3.1	Pre-Strain Experiments	36
3.3.2	Reversed Plastic Flow Experiments	36
3.3.3	Tensile Deformation of Foils	37
3.3.4	Preparation of Thin Films From Foils	38

Section	Subject	Page
3.3.5	Preparation of Thin Films from Bulk Specimens	38
3.4	Dislocation Density Determinations	40
3.5	Analysis of the Dislocation Density Data	43
4	Results	44
5	Interpretation of Results	46
5.1	Variation of Dislocation Density with Tensile Strain	46
5.2	Variation of Dislocation Density During Reversed Plastic Flow	49
5.3	Effect of Pre-strain on the Strain to First Jerk	51
5.4	Effect of Reversed Plastic Flow on the Strain to First Jerk	54
6	Discussion and Suggestions for Further Work	58
6.1	Variation of Dislocation Density During Reversed Plastic Deformation	58
6.2	Determination of the Rate of Vacancy Production During Reversed Plastic Deformation	59
6.3	A Detailed Study of Dislocations Before and After Reversed Plastic Deformation	60
7	Summary and Conclusions	61
Appendix A		
References		

LIST OF TABLES

Table	Contents
1	List of values of the index β of equation (9) determined from a re-analysis of previous work.
2	Results of all Dislocation Determinations.
3	Results of Pre-Strain Experiments on the Strain to First Jerk after Aging.

LIST OF ILLUSTRATIONS

Figure	Subject
1	Typical load-elongation curves found for a copper-3.2 at. % tin alloy at temperatures at which the P-L effect occurs. (Re-produced by kind permission of Dr. B. Russell).
2	Peiffer's results ⁽⁹⁷⁾ on the change in electrical resistivity during the interrupted tensile deformation of a copper specimen.
3	Logarithm of the mean dislocation density vs. logarithmic strain.
4	Logarithm of the flow stress increment vs. logarithmic strain.
5	Logarithm of the mean dislocation density vs. logarithm of the flow stress increment.
6	Hypothetical plot of logarithm of the dislocation density vs. logarithmic total strain, under conditions of reversed plastic flow.
7	Typical microstructure of specimen 22.
8	Typical microstructure of specimen 17.

SECTION I

Introduction

" Since the publication of Taylor's theory there has been no significant progress in the understanding of strain hardening."

E. Orowan, Conseil de Physique Solvay (1951)

This quotation may have been extended to embrace fatigue as well as strain hardening with no loss of accuracy.

Since the introduction of the concept of a dislocation a formidable volume of research work has been published on the subject and its ramifications and yet the basic difference between the deformation mechanisms of strain hardening and fatigue remains unsolved. The use of Electron Microscopy opened many doors, most of which concealed further problems to be solved.

A fundamental problem is that associated with difference between the microstructure of fatigued specimens and that of statically strained specimens, viz. a relatively high density of dislocation loops and debris in the former.

This is a very important feature which apparently results from a dislocation mechanism which is particularly active during fatigue.

What is the origin of this fatigue debris? Are the loops formed directly as the result of a dislocation intersection, or are they formed by the condensation of excess vacancies which were created by the deformation? The answers to these questions could be the keys to understanding the difference between the dislocation mechanisms which operate during fatigue and tensile deformation.

The evidence in support of the vacancy condensation mechanism is strong though inconclusive and is reviewed in detail in sections 2.1.3 and 2.1.4. It stems partially from the apparently enhanced diffusion rate of solute atoms in a specimen which has been subjected to many stress reversals and partially from the high density of dislocation loops observed in fatigued structures. Most of this evidence is suspect because only the end result is observable and it has not been possible to actually follow the processes step by step.

It was felt that an experiment which could actually indicate the concentration of vacancies during the early stages of fatigue and especially during the course of one fatigue cycle would be very enlightening. It was with this view that this project was undertaken.

Polakowski⁽¹⁾ and Russell⁽²⁾ have shown that primary solid solutions of a copper-tin alloy exhibit the Portevin-le Chatelier effect under certain conditions of temperature and strain rate. Russell has followed Cottrell⁽³⁾ in attributing the effect to the drag imposed upon mobile dislocations by solute atmospheres whose diffusion rate is greatly enhanced by the excess concentrations of vacancies produced during the tensile test.

Therefore the strain at the onset of the Portevin-le Chatelier effect in a copper - 3.2 at. % tin alloy should be a sensitive measure of the vacancy concentration. The effect has the virtue of occurring under dynamic loading conditions and thus is a true indication of the actual vacancy concentration at that stage of the deformation.

If a higher concentration of vacancies results from reversed stressing conditions, greater enhancement in the diffusion rate of tin atoms in the alloy should result. This would manifest itself as a decrease in the total strain (summed without regard to sign) necessary to initiate to Portevin-le Chatelier effect under any given set of conditions. Hence the rate of vacancy production during one fatigue cycle could be accurately determined by this method, provided these assumptions are correct.

The present work is an attempt to test the hypothesis that significantly more vacancies are produced per unit strain under reversed stressing conditions (fatigue) than during tensile deformation. It is also an attempt to measure the actual rate of vacancy production under these conditions.

SECTION 2

2.1 Production of Vacancies

2.1.1 Production of Vacancy Loops by Quenching, Irradiation, and Unidirectional Deformation

The presence of vacancies and interstitials in crystalline solids has long been accepted⁽⁴⁾. Thermodynamic arguments show that at any particular temperature there is an equilibrium concentration (C) of each of the point defects which is given by

$$C = \exp \frac{-(\Delta H_f - T\Delta S_f)}{kT}$$

where ΔH_f is the heat of formation of the defect

ΔS_f is the entropy change associated with the formation of the defect

T is the absolute temperature

K is the Boltzmann constant

At relatively low temperatures i.e., less than half the melting point of the solid, the concentration of defects is quite low but at temperatures near the melting point it is higher by several orders of magnitude.

The high energy of formation and the low energy of movement of interstitials cause them to diffuse very quickly to sinks at all but the very lowest temperatures. It is not thought that interstitials play an important role in metals⁽⁷⁾.

However, single vacancies and divacancies are much more stable in the lattice and markedly affect some physical properties of solids.

The case of vacancies in metals, particularly f.c.c. metals, has received extensive study over the last ten years^(5,6,7,8) since it is known that the mechanical properties of these metals are influenced by the presence of vacancies⁽⁹⁾. The equilibrium concentration of vacancies has little obvious effect on the mechanical properties but an excess of vacancies is able to modify them markedly.

An excess concentration of vacancies can be introduced into a metal by three methods.

- (a) Quenching the metal from a high temperature
- (b) Irradiation
- (c) Plastic Deformation. (In this section only unidirectional deformation will be considered).

(a) By quenching the metal from a temperature near its melting point to room temperature or below it is possible to supersaturate the metal with vacancies. The higher the quenching rate the greater the excess concentration of vacancies^(10, 11, 15). With very high quenching rates concentrations of up to 10^{-4} may be achieved.

(b) The bombardment of a non fissile metal with high energy neutrons produces vacancies and interstitials in concentrations far higher than the equilibrium concentration. The defects are formed at the extremities of the thermal spikes.

(c) The measurement of point defect sensitive properties such as density, electrical resistivity, and lattice parameters have shown that vacancies and perhaps interstitials are produced during unidirectional plastic deformation^(12,9). Friedel⁽¹³⁾ considers that equal numbers of vacancies and interstitials are produced by cold work. The relationship between the concentration of point defects and plastic strain has received considerable attention and is discussed in section 2.2.2.

At room temperature the single vacancies and divacancies are very mobile and seek lower energy configurations^(8,7,14,16,17,18,19). These have the form of a stacking fault tetrahedron, a perfect dislocation loop, or a dislocation loop containing a stacking fault^(8,14). The exact form depends on the stacking fault energy of the metal but in pure aluminium and copper perfect dislocation loops are the form⁽⁸⁾.

These loops are formed by the aggregation of vacancies into clusters and their subsequent collapse. In pure copper these changes occur in several stages between 250°K and 350°K⁽⁸⁾.

It is the loops and tetrahedra which interact with moving dislocations and cause irradiation hardening and quench hardening^(20,11,21).

During deformation the situation is complicated by the high density of dislocations which may act as vacancy sinks. It is probable that a fraction of the excess vacancies would condense to form loops, though a quantitative estimate is not available.

However, loops and dipoles are often seen in metals after plastic deformation and some direct evidence of their formation has been obtained^(22,23). It appears that they may be formed directly by the intersection of dislocations and the subsequent collapse of long unstable loops into smaller loops or dipoles.

The formation of dipoles during deformation is still a controversial topic^(24,25,44) but Fourie⁽²⁶⁾ has shown that both interstitial dipoles and vacancy dipoles are formed in copper.

There is no doubt that dislocation loops are formed by the condensation of vacancies, whatever their origin. These loops are the stable room temperature form in copper and aluminium. Interstitial dipoles are seen but interstitial loops have not been observed and are not thought to exist.

The presence of dislocation loops in quenched and irradiated metals is definite proof that the lattice was at one stage supersaturated with vacancies. The case of loops in deformed metals is less certain since it is possible that they may be formed directly as the result of certain dislocation interactions.

2.1.2 Theory of Vacancy Production During Fatigue

There appears to be little published work on this important aspect of fatigue. The subject has apparently been regarded as of secondary importance compared with the theory of vacancy production during unidirectional plastic flow.

However, Cottrell⁽¹²⁾ and Mott⁽²⁷⁾ have given the matter some consideration and conclude that fatigue should be a very efficient method of producing vacancies.

Cottrell⁽¹²⁾ considered the motion of a contracting dislocation ring which contains jogs. The jogs are thought to be able to glide backwards conservatively until the ring finally disappears, leaving a long dipole. He proposed that this may collapse to form a line of point defects. He presumes that the jogs are formed during the expansion or contraction of the ring as the result of intersections with closely spaced screw dislocations. Such a mechanism would be especially operative during fatigue.

Mott⁽²⁷⁾ and Friedel⁽¹³⁾ independently suggested another method for vacancy production. They proposed that a screw dislocation forms a loop around one or more screw dislocations which thread the glide plane. If there is an excess of screw dislocations of either sign in the forest the parts of the glide dislocation which would normally meet and annihilate cannot do so. Instead the parts would overlap and collapse to form a row of point defects and a jog in the dislocation. If the excess number of screw dislocations of one sign threading the glide plane exceeds unity, plates of point defects would be formed.

Mott⁽²⁷⁾ suggested that when the stress is reversed it is possible that the jog would overshoot its original point of formation and create defects of opposite type on the other side of the loop by a similar mechanism.

He also proposed that a similar mechanism could operate if the glide dislocation was held up by a previously formed dislocation loop instead of a forest of screw dislocations.

No quantitative work on these hypotheses seems to have been attempted and the suggestions have been purely speculative.

2.1.3 Evidence of Vacancy Production From Transmission Electron Microscopy

Dislocation loops and debris have been widely observed in f.c.c. metals (28,29,30,31,32,33,34,35,127,49) and in iron, niobium, and magnesium specimens (36,37) which have undergone a large number of cycles of fatigue. Among these workers there is some confusion as to effect of the stress level on the formation of loops. Grosskreutz and Waldow (29) found very few loops at "high" fatigue stresses in aluminium. Segall and Partridge (32) found the same tendency for a much higher density of loops to be formed at the "low" stress levels but still observed many loops formed by "high" stress level cycling, as did Snowden (30). This discrepancy does not pose a serious problem since Segall et al (33) found that a tensile strain imposed upon the fatigued specimen caused the glide dislocations to sweep up the previously formed loops.

Strudel and Washburn (18) have observed imperfect (i.e. containing a stacking fault) loops in aluminium formed by rapid quenching. They were always converted to perfect loops after an intersection with a moving dislocation. It seems reasonable to expect that loops formed

during high stress fatiguing may be swept up by moving dislocations which travel larger distances than their counterparts in low stress fatiguing. The loops appear to be a feature of the fatigue substructure right from the first cycle⁽³⁰⁾.

There may be a basic difference between loops formed at high and low strain amplitudes. Snowden⁽³⁰⁾ observed that loops formed at high strain amplitudes were not removed by further cycling at low strain amplitudes even though the specimen work softened.

Be this as it may, loops are seen in pure metals in abundance after fatigue. They are often closely associated with dislocation tangles and cell walls.

Feltner⁽³⁸⁾ has shown that the typical high density of loops is not observed in fatigued aluminium if there is no compressive component of alternating stress. A tension-tension fatigue test gives rise to a density of loops comparable with that resulting from straight tension. Hence an essential requirement for the production of a typical fatigue structure is the intersection of dislocations in a manner which would be unfavourable under conditions of tensile stress only.

A note of caution may be well placed at this point. The structures observed by transmission electron microscopy may not be truly representative of the actual bulk structure. This possibility has been recognized and studied^(39,40,41,42,43,44,45,46). Ham and Wright⁽⁴⁷⁾ have measured the loss of dislocations during the thinning of aluminium

to 2 microns by a resistivity method and have shown the loss to be about 80%. It is probable that further thinning to 2000 Å to 3000 Å would induce an even greater loss. It is also recognized that dislocation rearrangement may take place during thinning, especially in low melting point pure metals^(44,45,48,49). In alloys the loss and amount of rearrangement is expected to be much less because of the locking effect of the impurity atoms on the dislocations. In alloys which strain age strongly it is reasonable to assume that losses would be small and rearrangement negligible.

It has been suggested that screw dislocations would be preferentially lost⁽⁴⁵⁾ and it is possible that loops may be more susceptible, than other dislocation arrangements⁽⁴⁴⁾. Segall et al⁽³³⁾ have observed that in pure copper the loops annealed out in the temperature range 300°C to 400°C. The dislocation tangles and cell walls did not begin to anneal out at temperatures below 500°C.

Pelloux⁽⁴⁹⁾ has investigated the rearrangement of dislocations during thinning and observed that long loops tend to be pinched off to form smaller loops in copper and aluminium. However, smaller loops are absorbed by the larger loops, even at room temperature. He concludes that the overall density of loops does not change significantly.

Hirsch et al⁽⁵⁰⁾ have claimed that alloys of low stacking fault energy do not exhibit the normal high density of loops and debris associated with fatigue structures in pure metals. Segall and Finney⁽⁴⁰⁾

found very few loops in 70/30 brass specimens which had undergone high stress fatiguing, and virtually none in the low stress fatigued specimens.

However, careful electron microscopy by Pelloux⁽⁴⁹⁾ revealed that in the same alloy under the same conditions a high proportion of the dislocation structure was large and small dipoles. The debris was dense and evenly distributed throughout the structure. Swann⁽⁵¹⁾ observed similar structures in brass and Cu-Al alloys. Pelloux⁽⁴⁹⁾ found that the main difference between the pure metals, copper and aluminium, and the alloy, brass, was the complete absence of cell formation and the long rows of dislocation dipoles observed in the brass.

Waldron⁽³⁴⁾ found the usual high density of loops and jogged dislocations in Al-Mg alloy specimens which had been fatigued. Similar structures have been reported in age hardening alloys of Al-Cu and Al-Ag both in the solution treated condition and in the conditions where non-coherent or semi-coherent precipitates were present.^(52,53)

In summary, it appears that dislocation arrangements in alloys of low stacking fault energy differ from those in pure metals. However the feature of a high density of loops, dipoles and debris is a general feature of all alloys and does not depend on stacking fault energy or the magnitude of the fluctuating stress, provided the fluctuating stress has a compressive component.

2.1.4 Other Evidence

One of the earliest suggestions that fatigue seemed a very efficient method for producing vacancies was made by Broom and Ham⁽⁵⁴⁾ and Ham⁽⁵⁵⁾. They showed that copper fatigue hardened at 78°K to a certain level which was softer than the level it attained after a subsequent room temperature anneal. A specimen fatigued at room temperature showed no increase in hardness after a similar treatment. They proposed that large numbers of vacancies were produced by the fatigue process but at low temperatures (<170°K) the vacancies were trapped in the lattice. The subsequent room temperature anneal allowed the vacancies to coalesce to form loops and to diffuse to dislocations and other sinks. The resultant high density of loops and jogged dislocations were responsible for the rise in flow stress and the temperature dependence of the flow stress. This theory was consistent with known behaviour of irradiated f.c.c. metals⁽¹²⁾.

Their experiment has recently been repeated on pure copper in much greater detail by Johnson and Johnson⁽⁵⁶⁾ who used a new technique. They confirmed the findings of Broom and Ham and also measured the change in electrical resistivity during the fatigue tests. The total resistivity increase in the specimen fatigued at 4.2°K was five times greater than that in the specimen fatigued at room temperature. During the test at room temperature the dislocation density reached a saturation value of about $1.5 \times 10^{10} \text{ cm}^{-2}$ after 1% of the

expected life but the point defect concentration remained at its equilibrium value. Presumably, this is because the point defects are very mobile at room temperature and diffuse to sinks or form loops within a very short time of their formation. However, in the test carried out at 4.2⁰K the dislocation density reached a saturation level but the point defect concentration increased continuously with the number of cycles (N) according to the relationship

$$C_v \propto N^{1/4}$$

The equilibrium concentration of vacancies at the melting point of copper was reached after cycling for only 3% of the expected life so there can be no doubt that the effect was a substantial one. The one disturbing feature of this work was the results of identical experiments on O.F.H.C. copper. In these tests the electrical resistivity did not continue to increase after the first few hundred cycles as it did for the high purity copper specimen. This confirms the results of Rosenberg⁽⁵⁷⁾ who used direct electrical resistivity measurements. The reason for this impurity effect is not known.

The relatively poor fatigue properties of certain age hardening aluminium alloys have been attributed to a high vacancy production rate during fatigue. This was suggested by Broom et al⁽⁵⁸⁾ who considered that overaging or resolution occurred as the result of a vacancy-enhanced diffusion rate. This suggestion has been

misinterpreted.

substantiated recently by Clark and McEvily⁽⁵²⁾. They found that in Al-4% Cu and Al-15% Ag alloys heat treated to contain θ'' and, G.P. zones and γ' respectively, an aging process occurred during fatigue. In the former alloy the matrix contained bands deficient in θ'' after fatigue and in the latter alloy the fatigue process had accelerated the precipitation of γ' and γ . They considered that this could be due to a vacancy enhanced diffusion rate. This effect has also been observed in quenching experiments⁽¹⁷⁾ and irradiation experiments⁽⁵⁹⁾ where the solute diffusion rates were definitely enhanced by the presence of a large number of point defects.

On the basis of the evidence presented in this section there would seem to be ample proof that vacancies are produced at a higher rate during fatigue than during any other mode of deformation. It would seem logical to expect that such a large effect would be readily detected in self diffusion experiments. This is not so. Ruoff and Balluffi^(60,70) have reviewed all the experiments concerned with enhanced diffusion rates in f.c.c. metals under all modes of deformation and have concluded that much misleading information has been published and incorrectly interpreted and that there is no evidence of enhanced self diffusion due to deformation of any kind. This conclusion would appear to cast doubt on other evidence of high vacancy production rates during fatigue. However, Balluffi and Ruoff⁽⁷⁰⁾ do concede that any effects would be very localized, especially at low temperatures and their detection may require techniques of much greater sensitivity than have previously been used.

A theoretical examination of the effect of plastic deformation on diffusion rates has indicated that they are enhanced during deformation (128).

2.2 The Portevin-le Chatelier Effect

2.2.1 General Discussion

The Portevin-le Chatelier effect is often referred to as the phenomenon of "Jerky Flow" or "Discontinuous Yielding". The latter term, although widely used, is misleading because it is also used to describe the behaviour of metals which are given an interrupted tensile test. Therefore it is not favoured in this thesis.

The "Portevin-le Chatelier effect" is commonly and conveniently abbreviated to the "P-L effect" and this convention will be followed.

The effect was first recognized by Portevin and le Chatelier in 1923⁽⁶¹⁾. Since then its occurrence in a wide variety of alloys has been reported^(1,2,62,63,64,65,66,67,68,69,71,72,73,74,75,76,77,78,79,80,81,82). The effect does not occur in pure metals but only in metals containing certain interstitial or substitutional solute atoms. In b.c.c. metals low concentrations of carbon, nitrogen, hydrogen or oxygen may be sufficient to give rise to the effect. Among the f.c.c. metals certain primary solid solutions of Al-Mg, Al-Cu, Cu-Zn, Cu-Sn alloys and hydrogen charged nickel exhibit the effect.

The P-L effect occurs over a restricted range of temperature, strain rate, and composition. The three variables are interdependent and these restrictive relationships have been extensively studied.

Cottrell and Jawson⁽⁸³⁾ proposed that the effect could be explained in terms of "solute atmosphere" drag on the moving dislocations. Cottrell⁽³⁾ showed that their model was directly applicable to interstitial impurities in b.c.c. metals. However, the diffusion rate of substitutional solute atoms was far too low to account for the effect in f.c.c. metals at the temperatures at which jerky flow occurs. Cottrell⁽³⁾ proposed that the diffusion rate of the solute atoms is greatly enhanced by a large excess of vacancies created in the lattice by the deformation which occurs during the tensile test. This view also accounted for the smooth deformation after the initial yield which always precedes the first serration in the load-elongation curves of f.c.c. alloys.

Once this diffusion rate is achieved the individual solute atoms are able to diffuse through the lattice at a velocity comparable to that of moving dislocations. The solute atoms are attracted to the cores of the dislocations by both the shear and the dilatation components of the stress fields surrounding screw and edge dislocations. Thus, any solute atom which has sufficient elastic misfit energy is attracted to the dislocations. Once the solute atoms near the cores of the dislocations are able to diffuse as fast as the

average velocity of the moving dislocations, an asymmetrical solute atmosphere is formed around the dislocations. These atmospheres exert a retarding force on the dislocations and cause them to slow down. If the total strain rate is fixed the flow stress rises until a level is reached which causes dislocations to break away from their solute atmospheres and the process is repeated.

The repetition of the process and the subsequent alternation of dislocations between fast and slow average velocities results in the characteristic serrated load-elongation curve.

Cottrell⁽⁸⁴⁾ has estimated that the strain rate at which the P-L effect will occur is given by

$$\begin{aligned} \dot{\epsilon} &= \bar{v} \cdot b \cdot \rho \\ \text{i.e. } \dot{\epsilon} &= \frac{4D \cdot \rho \cdot b}{l} \end{aligned} \quad (1)$$

where \bar{v} is the average velocity of a moving dislocation

b is the Burgers vector

ρ is the dislocation density

D is the diffusion coefficient of the solute atoms in the alloy

and l is the effective radius of the solute atmosphere

The vacancy assisted diffusion coefficient of the solute atoms (D) can be expressed in terms of the vacancy concentration (C_v) by equation (2) which was suggested by Seitz⁽⁸⁵⁾ and Mott^(88,86)

$$D = a^2 \cdot V \cdot Z \cdot C_v \cdot \exp(-Q_m/kT) \quad (2)$$

where a is the lattice parameter

V is the Debye frequency for lattice vibration

Z is the coordination number

Q_M is the activation energy required to move a solute atom into a vacant lattice site

k is the Boltzmann constant

T is the absolute temperature

Under conditions of constant temperature, equation (2) reduces to

$$D = \text{const. } C_V \quad (3)$$

A combination of equations (1) and (3) gives

$$\dot{\epsilon} = \text{const. } C_V \cdot \rho \quad (4)$$

At the critical strain rate necessary for the occurrence of the P-L effect ($\dot{\epsilon}_{\text{crit}}$) equation (4) becomes

$$\dot{\epsilon} = \text{const. } C_V^1 \cdot \rho^1 \quad (5)$$

where C_V^1 is the critical concentration of vacancies to enhance the solute diffusion rate to the minimum level necessary to allow the solute atmosphere to catch the moving dislocation, and ρ^1 is the dislocation density at the strain at which the first jerk occurs.

It is generally accepted that the concentration of vacancies is a function of the plastic strain in f.c.c. metals. Seitz⁽⁸⁵⁾ suggested that vacancies would be produced according to the power law

$$C_V = B \epsilon^m \quad (6)$$

where B and m are constants for any particular metal. The validity

of equation (6) has been questioned and an alternative relation between the concentration of vacancies and the shear stress has been proposed by Akulov⁽⁹⁰⁾ and others.^(89,91)

Saada⁽⁹²⁾ also proposed a proportionality between the vacancy concentration and the plastic work viz.

$$C_v = \frac{A}{E} \int_0^{\epsilon} \sigma(\epsilon) d\epsilon \quad (7)$$

where $\frac{A}{E}$ is a constant and ϵ is the plastic strain. His prediction (equation (7)) has been verified for pure aluminium, gold, silver and copper and a number of their alloys.^(93,94,95)

It is noteworthy that the results of Pistorius⁽⁹⁴⁾ have been quoted as proof by both schools of thought on this subject. He offers his results as a verification of the Saada relationship between the concentration of vacancies (C_v) and the plastic strain. Kovacs and Nagy⁽⁹¹⁾ have reanalysed his results and claim they obey the Akulov type proportionality between C_v and the shear stress.

At first sight this may seem inconsistent but in the linear hardening region of f.c.c. metals at least, it is not so. In this region the shear stress is directly proportional to the plastic strain and therefore any quantity which is proportional to one of these variables is also proportional to the other. Hence both Saada's and Akulov's relationships would be expected to hold as long as the linear hardening behaviour exists.

One of the laws may be expected to fail at relatively high temperatures or in the very early or late stages of deformation.

These conditions all give rise to a non-linear hardening behaviour in the tensile specimen and thus the direct interdependence of the two relationships is lost.

Whatever the universally correct law may be it is satisfactory to assume that for a f.c.c. metal at low temperatures and during stage II deformation the concentration of vacancies varies with plastic strain according to a power law (i.e. $C_v \propto \epsilon^m$).

Seitz⁽⁸⁵⁾ measured a value of $m = 1$ for aluminium and Bolling⁽⁹⁶⁾ found an experimental value of $m = 1.36$ for brass. The results of Peiffer⁽⁹⁷⁾ can be reanalysed to yield a value of $m = 1$ for pure copper (Appendix A).

Edington et al⁽⁶⁷⁾ successfully predicted the temperature range of the P-L effect in impure vanadium by using Cottrell's equations and the impurity diffusion rate as determined from strain aging experiments.

These results serve to strengthen the validity of Cottrell's assumptions and his theory of the P-L effect in both f.c.c. and b.c.c. metals.

Some criticism of the Cottrell theory has arisen as the result of experiments on dilute aluminium alloys^(69,98). The classical theory predicts a linear relationship between the logarithmic strain to first jerk and the logarithmic strain rate and this relationship does not hold for dilute aluminium alloys.

If this were a real and general effect it would indeed be a very serious objection to the Cottrell theory. It is not a general effect because the results of Russell⁽²⁾ obey the classical prediction over a wide range of strain rate, temperature, composition and grain size.

Further, Sperry⁽⁷⁴⁾ has shown that dilute aluminium - magnesium alloys are peculiar in that they recover and soften at room temperature immediately after deformation, and in fact he suggests a new model for the P-L effect in these alloys based on this observation.

The reported deviations from the Cottrell prediction can be explained by recovery and softening which takes place during the test. This recovery results in a greater strain than normal at any particular stress value and this would manifest itself as a larger strain to first jerk than is predicted. Alternatively, if dislocations are annihilated during the softening process, equation (5) demands that the critical concentration of vacancies be increased if a given strain rate is maintained. This means that further strain is required to produce the extra vacancies and thus the strain to first jerk is greater than predicted.

The large discrepancies discussed by Bailey⁽⁶⁹⁾ and Harris⁽⁹⁸⁾ occur at the slowest strain rates and/or the higher temperatures. This is consistent with the recovery and softening explanation. It may be significant that their results for the room temperature tests at the faster strain rates ($5 \times 10^{-3} \text{ sec.}^{-1}$) do obey the Cottrell prediction.

It is concluded that the original theory of the P-L effect by Cottrell is valid; in aluminium alloys a correction must be made for recovery and softening which takes place during the test.

2.2.2 The P-L Effect in Cu-Sn Primary Solid Solutions

The occurrence of the P-L effect in Copper-Tin alloys was first reported by Polakowski⁽¹⁾. It and the strain aging behaviour of the alloys have since been extensively studied by Russell⁽²⁾, and Russell and Vela⁽⁹⁹⁾. Russell has shown that the Cottrell laws are obeyed in alloys of 1.1 to 6.9 at. % tin, at temperatures of 363^oK to 423^oK and at strain rates of $4 \times 10^{-5} \text{ sec}^{-1}$ to $3.25 \times 10^{-3} \text{ sec}^{-1}$.

While the previous thermal history of the specimens did affect the initial flow stress and the magnitude of the serrations it had no effect on the Cottrell relationships or the activation energy of the process.

The detailed structure of the experimental load - elongation curves he obtained is rather interesting. The serrations were completely regular and reproducible but differed slightly from some other published curves^(63,68,75,129,130). This difference may be due to the high sensitivity and accuracy of his experimental technique.

A set of typical load-elongation curves are reproduced with the kind permission of Dr. B. Russell in Figure 1. It can be seen that two types of serrations are present. The larger serrations (type A) first occur at lower strains than the other and appear throughout the remainder of the test. The smaller serrations (type B) are superimposed upon the type A serrations and the first one appears at a later stage in the test than the first of the type A jerks.

The type B jerks are commonly observed in other alloys but the type A jerks are usually less well defined. Russell has associated the type A jerks with the propagation of a Luder's band and the type B jerks with the motion of dislocations dragging solute atmospheres.

However, Russell⁽¹⁰⁰⁾ and the author (present work) have not been able to observe or detect the propagation of a Luder's band under normal conditions. This does not mean that Luder's bands do not propagate in the metal. The onset of plastic deformation is followed by a small plateau in the load-elongation curve and this is a definite indication that a Luder's band is associated with yield, but none was seen to be associated with this type of yield either.

Other workers^(63,75,82) have observed that the individual jerks are connected with the appearance of slip lines on the surface of the specimen. The exact nature of the slip lines is not clear and it seems to depend on the alloy. Ardley and Cottrell⁽⁶³⁾ found that each type A serration was associated with the appearance of a coarse, widely spaced, slip line whilst the type B jerks were associated with

fine slip lines which occupied the areas between the coarse lines.

The exact form of the yield may manifest itself in several ways but it is certain that the serrations are related directly to some sort of local or general deformation band. Russell⁽²⁾ has shown that for Cu-Sn primary solid solutions the strain between type A jerks is directly proportional to the instantaneous gauge length of the specimen. This strongly suggests the existence of deformation fronts which run the length of the crystal at the instant a type A jerk appears on the load-elongation curve.

Hahn⁽¹⁰¹⁾ has estimated that the velocity of free dislocations in f.c.c. metals is very high so it may not be possible to actually observe the propagation of a deformation front under such a condition.

The type B serrations are even less well understood, especially in Cu-Sn alloys. Russell proposed that they are due to the breakaway of individual dislocations situated within the deformation band during straining. It is difficult to reconcile this idea with the velocity of the deformation front. If the front is moving so quickly that its passage is not observable then the dislocations involved in its propagation should be moving at velocities far too high to allow dynamic strain aging to occur. It is clear that this aspect of the P-L effect is not well understood. It is certain that both types of jerks are the result of dynamic strain aging. Russell⁽²⁾

has shown that both serrations obey the Cottrell laws and have the same activation energies. It may well be that type A and type B jerks initiate simultaneously but that at the lower strains the load drop associated with a type B jerk is below the detection limits of the instrumentation.

In summary it may be said that although the details of the P-L effect in Cu-Sn alloys are not well understood the onset of the effect has been convincingly related to the process of dynamic strain aging. The details of how the jerks are repeated are not important, since the analysis can be limited to only the onset of the P-L effect. As a result it is possible to use the effect to measure the instantaneous concentration of vacancies created during plastic deformation, provided the relationship between the plastic strain and the dislocation density is known.

2.3 Dislocation Density as a Function of Stress or Strain

A basis for the study of the deformation of metals is that plastic behaviour can be explained in terms of dislocations. More specifically, plastic deformation at low temperatures is a consequence of the forced motion and multiplication of dislocations. Therefore, it is very important that, in considering any theory or experiment concerned with plastic deformation, the dislocation density and arrangement be known.

By means of transmission electron microscopy and etch pit methods these two variables may be determined with fair accuracy.

By utilizing these and other techniques the dislocation density has been determined as a function of the imposed stress and/or strain for some important metals^(102,103,104,105,106,107,108) and some ionic crystals^(109,110). In some cases the strain has been chosen as the independent variable and in others it has been the stress.

The various results are not consistent and confusion in the literature still exists. From the available data two empirical laws have evolved. The first is that relating the applied resolved shear stress (τ) to the observed dislocation density (ρ), as determined by Bailey and Hirsch⁽¹⁰²⁾ viz.

$$\rho = \text{const. } \tau^2 \quad (8)$$

This relationship has been experimentally verified for some f.c.c. metals and ionic crystals.^(103,104,105,107,109,111,95,112,113) Venables⁽¹¹⁴⁾ claims that his results obey equation(8)but the scatter is such that no confidence can be attached to them. A similar relationship has been found to hold for the increase in the applied resolved shear stress^(108,112,116) i.e. $\rho = \text{const } (\tau - \tau_0)^2$ (8A) where τ_0 is the initial resolved shear stress.

The second relationship is that between the dislocation density and the plastic strain (ϵ), as found by Lomer and Rosenberg⁽¹⁰⁶⁾ viz.

$$\rho = c\epsilon^\beta \quad (9)$$

This law has been found to hold for a wide variety of metals and alloys^(106,107,108,117). The value of index β varies among the metals but is commonly between 0.5 and 2.0 for f.c.c. metals⁽¹¹⁷⁾.

The other relationship of importance in this discussion is the one between stress and strain. In f.c.c. metals and alloys during stage II deformation a linear relationship exists; i.e.

$$\tau = \text{const. } \epsilon \quad (10)$$

This link-up of the three variables provides a method of checking the accuracy of these empirical laws. For example, Bailey and Hirsch⁽¹⁰²⁾ found that in polycrystalline silver equation (8) is obeyed. In the range of stress imposed on the specimens by them at room temperature linear hardening occurs and therefore equation (10) must hold. One can predict that the dislocation density should depend on strain according to the equation,

$$\rho = \text{const. } \epsilon^2 \quad (11)$$

This prediction and the results of Bailey and Hirsch have been verified⁽¹⁰⁷⁾. In this experiment the dislocation densities were determined by etch pit techniques on single crystals of silver, oriented for multiple slip.

A similar double relationship was found for tantalum^(108,110) but in this case the absolute value of the strain index, β , varied from 0.45 to 2.96. The index was sensitive to temperature, and the initial dislocation arrangement. However, the validity of equation (11) is not challenged here because under the testing conditions linear hardening did not occur.

Data published by other workers^(102,103,106,105,34) have been reanalysed by the author and in cases where multiple slip occurred equation (9) was applicable. However the values determined for β were not close to two. In all cases the values were below 1.30 and for some dilute aluminium alloys they were very low. All the values are listed in Table 1.

The reason for these low values is not understood though it is possible that a substantial proportion of the dislocations may have been lost during the preparation of the thin films.

The explanation of the general low values of β may lie in the strong strain aging characteristics of three of the metals^(106,34,68). They are all alloys which exhibit the Portevin-le Chatelier effect at the temperatures at which the tensile deformation was carried out. It is suggested that under these conditions the flow stress may not be dependent on the density of dislocations in the same manner as it is in pure metals.

However the results of Lomer and Rosenberg⁽¹⁰⁶⁾ have shown that this is not so for brass. Their results obey equation (8) and (10) but not equation (11) i.e. the dislocation density is not proportional to the square of the plastic strain. It is clear that a discrepancy exists in this case. However the values of the various indices may be uncertain enough to account for the difference of 0.7 in the value of β . Insufficient detail was available to allow an investigation of the accuracy of the results to be carried out.

The data of Bailey and Hirsch⁽¹⁰²⁾ and Bailey⁽¹⁰³⁾ were too limited to allow an accurate determination of β , and Hordon's⁽¹⁰⁵⁾ results were for single slip conditions where equation (10) does not hold.

In conclusion, it may be said that the published data for pure metals substantiates the three general equations relating stress, strain, and dislocation density. However the case of alloys is uncertain and it is possible that at least one of the three basic equations is not valid under certain conditions.

2.4 Annihilation of Dislocations During Reversed Plastic Flow

Since the early years of accurate fatigue research one of the unsolved problems has been the cause of the Bauschinger effect. If a tensile plastic strain is followed by compressive strain instead of another tensile strain plastic flow occurs during compression at a much lower absolute stress than it would during subsequent tension. Alternatively, if a specimen is prestrained in tension, unloaded, and then reloaded in tension or compression to some stress level, the compressive strain is greater than the tensile strain. Reversed plastic flow may even occur during the unloading of the tensile stress.

One explanation of this apparent anomaly is that untangled dislocations move back freely during the stress reversal and annihilate with dislocations of opposite sign. This would give rise to plastic flow at very small compressive stresses. This explanation is not widely held but has some support⁽¹¹⁸⁾.

Stored energy measurements have been carried out on pure copper specimens which have been strained in tension and subsequently compressed^(119,120). Specimens were pulled to approximately 30% strain, rested, and compressed various amounts. Both the hardness and the stored energy initially decreased, reached a minimum value, and then increased continuously thereafter as the compressive strain was increased. The minimum in each occurred after approximately 5% compressive strain. The dislocation density at this compressive strain was found to be only half that of the uncompressed specimens⁽¹¹⁹⁾. This result agreed with some preliminary work on copper single crystals done by Ham⁽¹²¹⁾. However in both cases the dislocation density was determined by transmission electron microscopy and it was feared that the drop in the dislocation density could have been due to dislocation losses incurred during the electrothinning procedure.

However, the results did indicate that dislocations may be annihilated during reversed plastic flow.

Although the strains involved in these experiments were much larger than those which occur during a fatigue cycle the basic tension plus compression components were present.

Recent work by Halford⁽¹²²⁾ on the stored energy changes which occur during a high strain torsional fatigue cycle has shown that a drop occurs during the initial reversed plastic flow in each half cycle. He has ascribed this loss to the annihilation of lattice defects, but he has no evidence that the defects are dislocations.

The evidence to suggest that dislocations are annihilated during reversed plastic flow is scant though encouraging. As far as the author is aware no contradictory evidence exists and the possibility has received little attention so far.

SECTION 3

Experimental Details

3.1 Materials and specimen Preparation

The material was kindly supplied by Dr. B. Russell in the form of 3/8" diameter swaged rod. The details of its preparation are reported elsewhere⁽²⁾. As received, the composition of the alloy was copper plus 3.2 at. % tin. The purity of the copper and tin are given elsewhere⁽¹²³⁾. During the course of the present work it became necessary to prepare more specimens. To achieve this with the minimum of delay and to prevent any systematic errors being introduced by compositional changes, used specimens of the original stock were remelted and cast into a bar. The specimens were all cleaned in concentrated nitric acid before melting. The melting was carried out in a graphite crucible by induction heating. One atmosphere of high purity nitrogen was maintained during the melting process. Just before casting the pressure was reduced to 0.1 atmospheres and the alloy was then quickly poured into a previously dried, warm, graphite mould. This was done to minimize evaporation of tin.

Because of the large volume of the mould compared with that of the alloy and the relatively high thermal conductivity of the

graphite, the metal solidified quite quickly and uniformly, in the shape of a half inch diameter rod. This procedure was adopted to minimize segregation and porosity during solidification.

The casting was cleaned in nitric acid, sealed under vacuum in pyrex glass tubing, and annealed for 70 hours at an actual temperature of 673°C . The casting was then rapidly quenched, cleaned and examined for casting defects. The top section did contain some defects and this section was discarded. Filings were taken from the cross section of the bar at different positions for subsequent chemical analysis. The analysis gave an average tin content of 3.2 at. % and no systematic variations in the bar were found. The cross section of the bar was etched and examined for segregation but none was seen.

The casting was then swaged down to 5/16" diameter rod with intermediate anneals under nitrogen.

From this rod, as from the original rod, parallel gauge length cylindrical tensile specimens were machined. Their dimensions were approximately as follows: parallel gauge length, 0.5": diameter, 0.17". Considerable variation in these dimensions was found. The specimens were annealed under nitrogen for two hours at 550°C and then water quenched to room temperature. All specimens were electropolished to ensure a standard surface finish. The dimensions of each specimen were measured by means of an optical comparator and marked on the specimen.

Foil specimens were prepared from the original bar by rolling a section of it to 0.003" thick sheet with intermediate anneals under

nitrogen. The direction of rolling was frequently changed to minimize the formation of a textured grain structure. Suitable specimens (approx. 1 1/2" x 1/2") were cut from the sheet with scissors. These specimens were clamped firmly between mild steel blocks and then the whole assembly was milled to a uniform width of 0.388". The foils were annealed with the bulk specimens.

3.2 Equipment

Specimens were strained in a T.T.C.L. model "Instron" adapted for reversed loading. This adapter also allowed the specimen to be completely immersed in a constant temperature bath. For a temperature of $140^{\circ}\text{C} \pm 1^{\circ}$, a thermostatically controlled bath of "Kyro-L" detergent was used.

Loads were measured by an "Instron" F.R. type load cell of 10,000 lbs. capacity. The machine was fitted with a standard "Instron" stepped zero suppression unit.

Special grips designed by D. F. Watt and Dr. R. K. Ham for reverse loading conditions were used throughout. These and the specimen mounting equipment have been described elsewhere⁽¹²⁴⁾.

For the foil specimens modified grips were used. Carefully matched half cylinders were clamped in the normal grips with the foil between the two half cylinders.

Slices for electrothinning were cut from the bulk specimens with a "Servomet" spark erosion machine. A fine molybdenum wire slicing adapter designed and built by Mr. M. L. Wayman was used to cut the slices.

Transmission Electron Microscopy was carried out on a Siemens Elmiskop 1, operated at 100 KV.

3.3 Experimental Techniques

3.3.1 Pre-strain Experiments

The aim of this set of experiments was to measure the effect of prestrain on the subsequent strain required to initiate the P-L effect at 140°C.

Specimens were pulled in tension at 140°C at a strain rate of 0.02 inches per inch per minute. The specimens were given various approximate pre-strains from zero to 3%. Each specimen was then unloaded, aged for sixty minutes at 140°C and restrained at the same temperature and strain rate until jerky flow occurred. The total extension was measured from the distance the chart had moved during the duration of the test. The elastic extension of the specimen, grips, adapter, etc. was subtracted from the total extension graphically. With a knowledge of the exact specimen gauge length, the true plastic strains were calculated for each specimen.

3.3.2 Reversed Plastic Flow Experiments

Two identical specimens were chosen for this experiment. Both were prestrained in tension at 140°C to about 3% strain, unloaded, and aged at 140°C for sixty minutes. Then one specimen was strained

in tension at 140°C until jerky flow began (specimen 22). The other was strained in compression until jerk flow began (specimen 17). Both were retained for dislocation density determinations. The specimen which was compressed (specimen 17) was checked carefully to ensure that it had not bent. Visual examinations did not detect any bending. The strain was also checked by measuring the distance between fine scratch marks on the specimen before and after straining by means of a travelling microscope. The compressive strain was found to agree closely with that determined from the chart travel. These two checks were accepted as proof that no bending had occurred during deformation.

Another specimen (specimen 23) was prestrained in tension, aged, and compressed in an identical manner at 140°C , except that in this case the compressive strain was only about 0.8%. Similar checks were carried out on this specimen but no bending was detected. It was also retained for dislocation density determinations.

3.3.3 Tensile Deformation of Foils

Five foils were deformed various amounts in tension of up to 8% strain at room temperature. Because the method of gripping was not entirely satisfactory some slipping within the grips did occur. Because of this, the extension within the specimen was measured directly. Two fine, parallel, pencil lines approximately 0.7" apart were marked on each foil prior to deformation. The distance between them was measured with a travelling microscope before and after deformation and the true plastic strain calculated directly. The foils were retained for dislocation density determinations.

3.3.4 Preparation of Thin Films From Foils

The technique was the relatively straightforward and conventional electrothinning technique. An area away from the edges and gripped regions was chosen and the remainder of the foil was masked with "Microstop". A modified Bollman technique was adopted. Sharp pointed stainless steel wires were used as cathodes.

The solution used was 25 vol. % nitric acid and 75% methanol. Electrothinning was carried out at -20°C at 10 - 12 volts and 0.3 amps.

Suitable thin areas were cut from the foil under methanol with a scalpel, dried, and mounted between grids in a standard Siemens holder.

The technique was dependable, simple and efficient.

3.3.5 Preparation of Thin Films from Bulk Specimens.

Slices were cut from the gauge length section of the bulk specimens, perpendicular to the length by a spark erosion method. Slices 0.030" to 0.060" in thickness were cut although the machine was capable of producing much thinner slices.

This was done for two reasons:

(a) The discs as cut had many surface ripples on them as a result of the slicing operation. It was found that if the slices were thinner than about 0.030", holes formed between the valleys of one side and those of the other during electrothinning. The areas around and between these

holes were much too thick for transmission electron microscopy. If thicker slices were used the ripples were removed by the thinning process before holes began to form and hence the chance of getting thin areas was greatly increased.

(b) The spark erosion process is known to produce a damaged layer at the surface of the disc⁽¹²⁵⁾. The layer may be up to 0.020" deep in pure copper.

It is imperative that these damaged layers be completely removed before thin films are obtained. In thin slices (approx. 0.010") this would certainly not have been accomplished and even slices about 0.030" thick may have damaged areas near the centre, if the metal were pure copper. However, it is expected that the damaged layer is much shallower in Cu-Sn than it is in pure copper. Therefore the thin films obtained from 0.030" to 0.060" thick discs of Cu-Sn alloy were considered to be free of damaged material.

The slices were cleaned by immersion in concentrated nitric acid for two to three seconds, followed by a methanol wash. To produce thin films from the discs, a modified "window" technique was developed.

The edges of the discs were protected with "Microstop" while the centre portion was extensively polished. The "Microstop" was then removed and the whole disc was thinned. This process was repeated as often as necessary to produce a thin area between two small holes. The two-step procedure was necessary to prevent extensive edge thinning which occurred on the unprotected edges of the slices and to prevent excessive

local pitting which occurred adjacent to the edge of the "microstop". With frequent repetition of this two-step process and care it was possible to uniformly polish most of the disc. However, the technique was not entirely successful and only about 25% of the discs thinned in this manner yielded useful thin films. It was therefore necessary to have an ample supply of discs from each of the bulk specimens. The same nitric acid-methanol solution was used at -20°C and 10 - 12 volts but about 3.0 amps were required to achieve the electrothinning condition.

3.4 Dislocation Density Determinations

Preliminary observations of the dislocations within the foils by transmission electron microscopy had shown that their density varied quite widely (by a factor of 10) between grains and often even within one grain. It was therefore necessary to ensure that the areas of each foil which were photographed were a representative sample of foil. A standard technique was developed and used for each thin film examined.

All areas in which dislocations were clearly visible were photographed. If more than one plate was required to accomplish this (as it often was) sufficient plates were exposed to cover the whole area. Areas which had no visible dislocations in them were tilted until the dislocations become visible and the best contrast was obtained. All thin areas in each thin film were treated in this manner. (Any areas

of the films which were bent after thinning were avoided.) Sufficient thin films were produced to ensure that the number of plates taken on any one foil was approximately forty. This number was a convenient compromise, since in work of this sort a great number of samples gives a higher level of confidence in the experimentally determined mean dislocation density, but the tedium of counting the dislocations and calculating the density is increased.

The dislocation density of each plate was determined by the intersection method of Ham⁽¹²⁶⁾. On plates where the number of intersections was greater than one hundred per twenty five centimetres of random line, enlarged prints were made of each plate and these were used for the dislocation density determination. Where the number of intersections was less than one hundred they were counted directly on the plate. Two such counts were made on each plate and the average was used in the dislocation density determination.

It is considered that the loss of dislocations due to thinning in this alloy is very small. Since the alloy is one which strain ages very strongly even at room temperature it is reasonable to assume that the dislocations were firmly held by condensed solute atmospheres after several days at 25°C or higher. This assumption would appear to be supported by the experiments of Waldron⁽³⁴⁾ on the strain aging Al-Mg alloys.

The dislocations were certainly observed to be securely locked in all the thin films examined during this work. Only those very short dislocations very near thin edges of the film could be induced to move in the electron microscope by the usual methods.

This caused a problem in the determination of the thickness of the areas examined in the foils. Often the dislocations could not be made to move so that a slip trace was not obtained. This meant that the slip trace method of film thickness determination could not be used. This was realized during the preliminary work on this alloy and so a standard method of estimating the film thickness by eye was adopted. Each area of interest was examined under the same conditions of magnification, filament current and filament bias. The relative intensity of the transmitted beam was used to estimate the film thickness within five arbitrary ranges viz. thin, thin to medium, medium, medium to thick, thick. The length of dislocations and their clarity also were considered when an estimate of the thickness was made. Whenever possible, the number of extinction fringes in each area was also noted.

The average number of extinction fringes associated with any particular arbitrary thickness range was calculated and the corresponding thickness found. The extinction distance of the alloy was assumed to be that of pure copper. It is considered that this assumption was completely justified since the atomic number of the alloy is 29.7 compared with 29.0 for pure copper. Even Ni, whose atomic number is 28 has extinction distances which are within the 10% accuracy of those for copper.

There are two major deficiencies in this method of thickness estimation.

(a) The extinction distance is a function of the reflecting lattice planes. The higher indexed planes have a greater extinction distance. For this analysis the average extinction distance of the main reflecting planes was taken.

(b) The transmitted intensity of the electron beam is also dependent on the orientation of the foil for any foil thickness.

In the determination of a single thin film thickness these factors could introduce a very serious error. However over a large number of estimates the errors should be completely random and lead to very little systematic error.

Hence the mean dislocation density of each foil as determined by this method is considered to be representative of the actual dislocation density and the errors in each value to be small and random. Proof of these assumptions is offered in section 5.1.

3.5 Analysis of the Dislocation Density Data

The dislocation density was determined for each plate and the mean dislocation density for each foil or bulk specimen was found. The standard error of each mean was also calculated. All calculations were checked.

It was necessary on several occasions to test the significance between two dislocation densities. This was done by carrying out a "Student's t" test on the relevant data in the standard manner.

SECTION 4

Results

All the data relevant to the dislocation density determinations are given in Table 2. This includes the number of dislocation density determinations done on each sample and the temperature of deformation, the deformation history, the mean dislocation density, and the standard error of the mean dislocation density of each sample.

The results are plotted in figure 3. The error bars shown in figure 3 are derived in two ways:

(a) The strain error bars are the experimental limits of the true plastic strain imposed on each specimen. Where these are not shown they are too small to be plotted.

(b) The mean dislocation density error bars were derived from the standard error of each value. The magnitude of each bar is the magnitude of 2.0 standard errors of the particular dislocation density. The value 2.0 was approximately the value which defined the 95% confidence limits for samples of size 30 to 70. The errors introduced by assuming a constant value of 2.0 for all samples are negligible. This means that there is a 95% chance that all values lying within these limits arose from the specimen whose mean dislocation density is given.

Figure 4 shows that there is a linear relationship between the logarithmic values of the plastic strain and the logarithmic values of the flow stress increment at 140°C. These results were derived from an actual true stress-true strain curve of a specimen deformed in tension at 140°C. The value of σ_0 , the flow stress at zero-strain, was found by extrapolation on a flow stress-strain plot.

Data taken directly from figure 3 and the actual true stress-strain curve at 140°C were used to construct figure 5. The analysis could only be carried out for strains up to 3.5% since at higher strains the P-L effect interfered.

Table 3 has the results of the experiments on the effect of pre-strain on the subsequent strain to first jerk at 140°C in both tension and compression.

Figures 7 and 8 are transmission electron micrographs of thin films of specimens 22 and 17 respectively. Each shows the typical substructure observed in thin films of the particular specimen.

The results of the "Students' t" tests are given and discussed in the relevant subdivisions of section 5.

SECTION 5

Interpretation of Results

5.1 Variation of Dislocation Density with Tensile Strain

Figure 3 shows the manner in which the dislocation density varies with the plastic strain during tensile deformation at 25°C. Four of the five results fit a straight line very well but the fifth does not. The reason for this is not known but it is considered to be due to experimental error.

It is possible that the points could lie on two straight lines. This would be feasible if cross slip was initiated at these low strains. The point of intersection of the two lines would mark the strain at which cross slip began at 25°C. However previous work⁽¹²³⁾ has shown that cross slip is not initiated in this alloy at 25°C at strains below 10%. Hence the cross slip explanation is not valid and there appears to be no reason why the points should not be fitted to a single straight line.

The slope of the straight line in figure 3 is numerically equal to the value of the index, β , of equation (9). This value was found to be 1.17 ± 0.13 i.e., the dislocation density was found to vary with strain according to the power law,

$$\bar{\rho} = \text{const. } \epsilon^{1.17 \pm 0.13} \quad (12)$$

This value of $\beta = 1.17$ agrees quite well with the value determined for 70/30 brass⁽¹⁰⁶⁾. This is the only copper based strain-aging alloy for which results were available.

Previous work⁽¹²³⁾ has shown that for strains below 10% at 25°C the flow stress increment is directly proportional to the plastic strain, within experimental error; i.e.

$$\sigma - \sigma_0 = \text{const } \epsilon^{1.0} \quad (13)$$

Figure 5 reveals that at 25°C the dislocation density is related to the flow stress increment according to equation (14), viz.

$$\bar{\rho} = \text{const. } (\sigma - \sigma_0)^{1.23 \pm 0.06} \quad (14)$$

This relationship differs from the more general relationship (equation (8A)) found by other workers^(108,112,116). The reason for this discrepancy is not known but the validity of equation (14) has been substantiated. The three basic equations relating stress, strain, and dislocation density have been determined experimentally and are consistent within experimental error. This is accepted as proof of the validity of equations (12) and (14).

The results of the dislocation density determinations on specimen 22 may be used to check whether equation (12) holds at a deformation temperature of 140°C. If it does hold, the value of the dislocation density of specimen 22 should fall on the straight line in figure 3. The plastic strain would be the sum of the plastic strains imposed on the specimen before and after the aging treatment.

It can be seen in figure 3 that the point for specimen 22 falls above the line i.e. its dislocation density is higher than that predicted by equation (12). To test whether the difference was significant or not a "t" test was carried out on the results of specimen 22 and foil 6.

Since foil 6 and specimen 22 had been strained approximately the same amount and since the point representing foil 6 lay directly on the line it was convenient to test the difference between their mean dislocation densities. The "t" test revealed that the difference was significant at the 10% level but not at the 5% level. This means that there is less than a 10% chance that the dislocation density of specimen 22 obeys equation (12). This is not a highly significant result and it cannot be said with any certainty that equation (12) is not valid at 140°C.

However, if it is tentatively assumed that the rate of dislocation multiplication is higher at 140°C than at 25°C, it is possible to determine the approximate relationship between the dislocation density and the strain. The dislocation density at zero strain may be assumed to be the same at both temperatures. A line may be drawn between the logarithmic value of the initial dislocation density and the logarithmic value of the dislocation density of specimen 22. The slope of this line is numerically equal to the value of β at a temperature of 140°C. A value of $\beta=1.27$ was determined from figure 3. This value lies with the experimental errors

of the value of β determined at 25°C.

Therefore, the difference between the dislocation density of specimen 22 and that predicted by equation (12) is considered to be due to experimental error and equation (12) is assumed to be valid at 140°C.

In section 3 the method of thin film thickness determination was described. It was assumed that the method would give small systematic errors and that the mean dislocation density would be representative of the sample, with a high degree of confidence. These assumptions are verified by the small magnitude of the standard errors of the mean dislocation densities (see Table 2). In all cases the standard error is less than 7.5% of the density. This is quite small for dislocation density determinations.

5.2 Variation of Dislocation Density During Reversed Plastic Flow

It has been suggested⁽¹¹⁸⁾ that dislocations may be annihilated during compression after tension and there have been indications that this may be so^(119,121). If this suggestion is true the dislocation densities of those specimens which had been subjected to reversed plastic deformation (viz. specimens 23 and 17) would be expected to be lower than the values predicted by equation (12). (In this case ϵ is the total strain summed without regard to sign).

Figure 3 reveals that this is so and in both cases the differences are significantly different at the 0.1% level. However this is not definite proof that dislocations were annihilated during the reversed plastic flow. If dislocations were produced at a lower rate during compression after tension than during either straight tension or straight compression the same results would be expected.

Specimen 23 had been strained 3.812% in tension and subsequently compressed to 0.798% strain. If the dislocation density after the total deformation was significantly less than the value predicted by equation (12) for 3.812% strain, definite proof of annihilation of dislocations would exist. The predicted dislocations density was higher than the value experimentally determined for specimen 23 ($9.85 \times 10^9 \text{ cm}^{-2}$ cf $9.56 \times 10^9 \text{ cm}^{-2}$) but it was not significantly so.

The differences are not attributable to the loss of dislocations during specimen thinning since the dislocations are strongly locked by condensed solute atmospheres in this alloy at room temperature.

Figures 7 and 8 show dislocation arrangements and distributions typical of all thin films which were examined in the electron microscope. The dislocations were evenly distributed within each grain and very little evidence of cell formation was seen. This is in keeping with the results of Swann⁽⁵¹⁾ and Pelloux⁽⁴⁹⁾ on low stacking fault energy alloys. All areas examined were entirely single phase and no evidence of solute segregation was observed.

The only systematic difference observed between any of the thin films was in the dislocation density. However no investigation of the detailed character of the dislocations themselves was attempted.

In summary it may be said that no definite proof that dislocations are annihilated during reversed plastic flow was found. However equation (12) does not apply during compression after tension and this means that either dislocations are annihilated during the initial reversed plastic deformation, or the rate of dislocation multiplication during compression after tension is lower than it is during straight tension.

Further work is required before the correct answer is known. (see section 6)

5.3 Effect of Pre-Strain on the Strain to First Jerk

Table 3 shows the results obtained from the experiments on the effect of pre-strain on the subsequent strain required to initiate the P-L effect at 140°C. For the sake of brevity the following abbreviations will be used in the remainder of this thesis.

ϵ_{Pre} - pre-strain before aging.

ϵ_{A} - strain to first jerk after aging.

ϵ_{Tot} - total strain before and after aging, summed without regard to sign.

From Table 3 it can be seen that as ϵ_{Pre} increases, ϵ_{Tot} increases and ϵ_A decreases. This general effect may be explained in terms of the Cottrell theory of the P-L effect. During the pre-straining, the dislocation density and the vacancy concentration increase according to equations (12) and (6) respectively.

During the aging treatment the dislocation density remains constant but C_v decays to the equilibrium value (≈ 0) by the diffusion of vacancies to sinks.

The dislocation density continues to increase during straining after ageing and the concentration of vacancies once more increases according to equation (6).

$$\text{i.e. } C_v = \text{const. } (\epsilon_{Tot}^m - \epsilon_{Pre}^m)$$

Therefore, at the strain at which the first jerk occurs, the following relationships must hold.

$$\rho = \text{const } \epsilon_{Tot}^{1.17 + 0.13} \quad (15)$$

and

$$C_v = \text{const } (\epsilon_{tot}^m - \epsilon_{Pre}^m)$$

Now at this point of deformation Cottrell's theory demands that the product ($\rho.C_v$) be proportional to the critical strain rate, $\dot{\epsilon}$.

Hence

$$\dot{\epsilon} = \text{const } \rho.C_v = \text{const. } \epsilon_{Tot}^{1.17} \cdot (\epsilon_{Tot}^m - \epsilon_{Pre}^m) \quad (16)$$

must apply at any particular strain rate and temperature. If the pre-strain is zero (i.e. $\epsilon_{Pre} = 0$) then equation (16) reduces to

$$\dot{\epsilon} = \text{const. } \rho \cdot C_v = \text{const. } \epsilon_{\text{Tot}}^{(1.17 + m) \pm 0.13} \quad (17)$$

Under the condition of zero pre-strain equation (17) may be applied to the results of Russell⁽²⁾. He used the strain to first jerk in the absence of pre-strain, ϵ_0 , to estimate the rate of vacancy production and found a value of 2.2 ± 0.1 for the total index of equation (17). (In the absence of pre-strain, $\epsilon_{\text{Tot}} = \epsilon_0$.) However, in his analysis of the data he assumed that the critical strain rate at the onset of the P-L effect is proportional to the concentration of vacancies only. This implies that the dislocation density is essentially constant at the first jerk under all testing conditions. This is not a valid assumption since the critical strain rate depends also on the dislocation density which in turn has been shown to depend on the strain.

His assumption lead him to equate his value of 2.2 ± 0.1 to m . This is wrong since equation (17) shows that the slope of the line in a plot of $\log \dot{\epsilon}$ versus $\log \epsilon_0$ is numerically equal to $(m + 1.17)$. By a combination of Russell's results and equation (17) a value of $m = 1.03 \pm 0.23$ may be determined.

It is possible to check equation (15) by an analysis of the results given in Table 3 in the following manner. Since $m = 1.03$, equation (16) may be rewritten as

$$\dot{\epsilon} = \text{const. } \epsilon_{\text{Tot}}^{1.17} \cdot (\epsilon_{\text{Tot}}^{1.03} - \epsilon_{\text{Pre}}^{1.03})$$

At a constant strain rate, this relationship reduces to

$$\text{constant} = \epsilon_{\text{Tot}}^{2.2} - \epsilon_{\text{Tot}}^{1.17} \times \epsilon_{\text{Pre}}^{1.03} \quad (18)$$

The values calculated for the constant of equation (18) after different amounts of pre-strain are given in Table 3. They are all approximately equal with no systematic variation between them and they agree quite well with the value of $\epsilon_0^{2.2}$, which is the limiting value for $\epsilon_{\text{Pre}} = 0$.

This agreement is taken as proof of the validity of equations(15) and of the accuracy of value $n = 1.03 \pm 0.23$.

Hence it has been shown that under the testing conditions described previously the concentration of vacancies is related to the strain according to the relationship

$$C_v = \text{const } \epsilon^{1.03 \pm 0.23}$$

This relationship is in good agreement with those predicted and experimentally determined by other workers^(13,85,96) for f.c.c. metals. These results are also considered to verify Cottrell's theory of the P-L effect.

5.4 Effect of Reversed Plastic Flow on the Strain to First Jerk

It has been suggested (section 2.1.2, 2.1.3, and 2.1.4) that reversed plastic flow, the essential element of fatigue, is a

highly efficient method of vacancy production. If this is true it should follow that ϵ_A should be much smaller in compression than in tension, after a tensile pre-strain, all other factors being equal.

Table 3 shows that this is not so and in fact after the same tensile pre-strain, ϵ_A in compression is more than twice the value found in tension. From this it could be inferred that reversed plastic flow is only half as efficient a method of producing vacancies as straight tensile deformation. However the difference between the dislocation densities of specimens 17 and 22 must be taken into account. Both specimen 17 and specimen 22 were unloaded shortly after the first jerk was observed and so the increase in dislocation density in each specimen after the first jerk would be small. It was possible to correct for the extra strain imposed after the first jerk in each case. Since these strains were accurately known, the corresponding dislocation densities could be calculated from equation 12. For specimens 22 and 17 the corrections were $1.60 \times 10^9 \text{ cm}^{-2}$ and $2.26 \times 10^9 \text{ cm}^{-2}$ respectively. Hence at the exact strain at which the first jerk occurred the dislocation densities were $17.83 \times 10^9 \text{ cm}^{-2}$ and $14.16 \times 10^9 \text{ cm}^{-2}$ for specimens 22 and 17 respectively.

In calculating the correction for specimen 17 it was assumed that equation (12) applied during the later stages of compression. This may not be true though it does seem a reasonable approximation for this particular case. In this instance the compressive strain was larger than the tensile pre-strain (4.5% cf 3.4%) and it

seems reasonable to assume that at this stage dislocations are being produced according to equation (9). Since the extra strains after first jerk are small, the corrections are relatively insensitive to the value of β provided it lies between 1.0 and 2.0. Hence it is considered that the corrections applied to the dislocation densities of specimens 17 and 22 are valid in both cases within experimental error.

A "t" test on these two corrected dislocation densities showed that the difference between them was just significant at the 5% level. (The variance of the uncorrected dislocation density was assumed in each case.) Considering the errors which may have been introduced in assuming that equation (12) applied during compression the difference is not highly significant.

At the strain at which the first jerk occurred in both specimens equation (5) must apply. Therefore

$$(\rho \cdot C_v)_{\text{Spec 22}} = (\rho \cdot C_v)_{\text{Spec 17}} = \text{constant}$$

Now since the dislocation densities of specimens 22 and 17 at ϵ_A are not significantly different, neither are their concentrations of vacancies.

$$\text{i.e. } (C_v)_{\text{Spec 22}} \approx (C_v)_{\text{Spec 17}}$$

Equation (6) may be assumed to be valid for both cases and since ϵ_A in compression is more than twice the value of ϵ_A in

tension, after the same pre-strain, it follows that reversed plastic flow produces approximately half as many vacancies per unit strain as straight tensile deformation.

The value of the index, n , could not be determined from the available results since the values of the constant B under these conditions was not known.

SECTION 6

Discussion and Suggestions for Further Work

6.1. Variation of Dislocation Density During Reversed Plastic Deformation

The results given in Table 2 and Figure 3 and discussed in section 5.2 have shown that either dislocations are annihilated during reversed plastic flow or they are produced at a lower rate in compression after tension than they are during straight tensile deformation.

The confusion could be eliminated by determining the relationship between the compressive strain and the dislocation density after any given tensile pre-strain.

Since the dislocation density does increase during compression after a tensile pre-strain it should be relatively simple to measure the actual relationship experimentally.

Whether dislocations are annihilated or not during reversed plastic flow could easily be determined once this relationship was known, by the following method.

It is logical to assume that the dislocation density versus total strain on a log-log. scale would be similar to that shown in figure 6. The presence of the minimum BDE pre-supposes that dislocations are annihilated during the initial reversed plastic flow. This would mean that two conflicting processes are in operation during this stage:

(a) the annihilation of dislocations according to the law defined by the line BZ.

(b) the multiplication of dislocations during compressive deformation according to the relationship defined by line EF. The slope of the line EF would be numerically equal to the value of the index β of equation (9) under conditions of reversed plastic flow.

If the minimum BDE was absent, this would be definite proof that dislocations are not annihilated during reversed plastic flow.

It may be experimentally difficult to detect the minimum even if it did exist. However, if the line EF, extrapolated to lower strains, intersected the line AB at B, the same conclusion could be drawn. If the point of intersection lay between B and A this would be definite proof of annihilation of dislocations.

If a minimum was found it would be very instructive to know the manner in which the strain at point D was related to the tensile pre-strain. Such a relationship would be useful in applying the results to actual fatigue experiments where the strains are usually much lower.

6.2 Determination of the Rate of Vacancy Production During Reversed Plastic Deformation

In section 5.4 it is shown that, per unit strain, reversed plastic deformation is a poor method for the production of vacancies

compared with straight tensile deformation. Had the exact values of the parameter, B , of equation (6) been known under the conditions of the experiments, the value of the index m could have been determined from the results of the present work.

It is possible that these values could be determined by other techniques such as electrical resistivity measurements and if so they would be very useful in analyses of the kind just described.

6.3 A Detailed Study of Dislocations Before and After Reversed Plastic Deformation

It has been suggested that dislocations may be annihilated during compression after tension and it has been shown that under this condition fewer vacancies are produced per unit strain than under the condition of straight tensile deformation.

A detailed study of the character of the dislocations and the type of dislocation intersections which occur could reveal information which would be useful in reaching an understanding of these effects.

SECTION 7

Summary and Conclusions

(a) The mean dislocation density was found to vary with the true plastic tensile strain at 25°C and 140°C according to the relationship,

$$\rho = \text{const. } \epsilon^{1.17 \pm 0.13}$$

This compares favourably with the similar relationship found for 70/30 brass by Lomer and Rosenberg⁽¹⁰⁶⁾.

(b) The mean dislocation density was found to vary with the flow stress increment according to the power law

$$\rho = \text{const. } (\sigma - \sigma_0)^{1.23 \pm 0.06}$$

This relationship differs from the accepted law for other metals but is consistent with the relationship between the mean dislocation density and the tensile plastic strain over the linear hardening range of tensile deformation.

(c) The relationship between tensile plastic strain and mean dislocation density does not hold under conditions of reversed plastic deformation. The discrepancy is attributed to the annihilation of dislocations or to the lower rate of production of dislocations during reversed plastic flow. It was not possible to distinguish between the two with the available results.

(d) No general difference in the arrangement or the distribution of dislocations was observed to exist between any of the samples examined in the electron microscope. The dislocations were generally evenly distributed and did not exhibit a strong tendency towards cell formation. This is in keeping with the findings of Pelloux⁽⁴⁹⁾ and Swann⁽⁵¹⁾ on alloys with a low stacking fault energy.

(e) The results of the pre-strain experiments were combined with the re-interpreted results of Russell⁽²⁾ to show that the concentration of vacancies varies with strain, for this alloy under the given experimental conditions, according to the relationship

$$C_v = \text{const. } \epsilon^{1.03 \pm 0.23}$$

(f) At 140°C compressive deformation after a tensile pre-strain is only half as effective in producing vacancies per unit strain as is tensile deformation after the same pre-strain. From this it is concluded that fatigue is less effective in producing vacancies per unit plastic strain than is straight tensile deformation. If a very large number of vacancies are produced by fatigue it can only be because of the large total plastic strain which may be imposed on a fatigue specimen before fracture.

APPENDIX A

Peiffer experimentally determined the change in electrical resistivity with tensile strain in copper at 78°K. At several stages during the test the specimen was removed from the low temperature environment, aged at room temperature for several hours, and then strained once more at 78°K. His results are illustrated graphically in Figure 2.

Because of the nature of the test he performed it is possible to separate the contributions due to dislocations and to point defects. Clareborough et al⁽⁸⁾ have shown that single vacancies and divacancies in pure copper, gold and silver aggregate to form clusters at temperatures between -20°C and 80°C.

Thus it is plausible to assume that the drop in resistivity after room temperature anneal is due to the annihilation of the point defects which were produced during the deformation at 78°K. The total resistivity can be divided into components due to dislocations and due to vacancies by graphical means. After a plastic strain ϵ_1 the total increase in resistivity is AB. Of this, BE is due to point defects and AE is due to dislocations. Similarly the other sections of the curve can be so divided.

64

By plotting the increase in resistivity due to vacancies only (ΔR_{vac}) against the plastic strain increment the law relating the the concentration of vacancies and the plastic can be found. ($C_v \propto \Delta R_{\text{vac}}$) The second and third sections of Peiffer's published curve were analysed in this way. Each section was treated as though the previous strain was zero. The initial section was not amenable to this analysis because line AE could not be drawn straight. This discrepancy may have been due to a non uniform rate of dislocation increase or to an error in the initial resistivity measurement.

However, the second and third sections of the curve were satisfactory.

From a log ΔR versus log $\Delta \epsilon$ plot the following relationships were determined.

Section 2

$$C_v (\propto \Delta R_{\text{vac}}) \propto \Delta \epsilon^{1.0}$$

Section 3

$$C_v (\propto \Delta R_{\text{vac}}) \propto \Delta \epsilon^{1.0}$$

In all cases the straight line of best fit could be drawn through the plotted points visually with good accuracy.

REFERENCES

1. Polakowski N.H., J. Inst. Met. 81, 601, (1952-53).
2. Russell B., Phil Mag. 8 615, (1963).
3. Cottrell A.H., Phil. Mag. 44, 829, (1953).
4. "Symposium on Vacancies and Other Point Defects in Metals and Alloys", Inst. Met. Monograph No. 23, (1958).
5. Simmons R.O. and Balluffi R.W. Phys. Rev. 117, 52, (1960).
6. Simmons R.O. and Balluffi R.W. *ibid* 119, 600, (1960).
7. Simmons R.O. and Balluffi R.W. *ibid* 129, 1533, (1963).
8. Clarebrough L.M., Segall R.L., Loretto M.H., and Hargreaves M.E., Phil. Mag. 9, 377, (1964).
9. Broom T. and Ham, R.K., "Vacancies and Other Point Defects in Metals and Alloys" p.41, Inst. Met. Monograph No. 23, (1958).
10. Wintenberger M.M., *ibid* p.201.
11. Meshii M. and Kauffman J.W., Acta. Met. 7, 180, (1959).
12. Cottrell A.H. "Vacancies and Other Point Defects in Metals and Alloys", p.1, Inst. Met. Monograph No. 23, (1958).
13. Friedel J., "Les Dislocations" (Gauthier Villars, Paris) (1956).
14. Thomas G. and Washburn J., Rev. Mod. Phys. 35, 992, (1963).
15. Brown N., Acta Met. 7, 210, (1959).
16. Manintveld, J.A., Nature, 169, 623, (1952).
17. Davies A.L. and Nicholson J.E., J. Inst. Met. 93, 109, (1964-65).
18. Strudel J.L. and Washburn J., Phil. Mag. 9, 491, (1964).
19. Seidman D.N. and Balluffi R.W., *ibid*, 10, 1067, (1964).
20. Galligan J. and Washburn J., Phil. Mag. 8, 1455, (1963).

21. Kimura H., Maddin R., and Kuhlmann-Wilsdorf D., *Acta Met.* 7, 145 (1959).
22. Price, P.B., *Phil. Mag.* 5, 873, (1960).
23. Fourie J.T. and Wilsdorf H.G., *J. App. Phys.* 31, 2219, (1960).
24. Nabarro F.R.N., Basinski Z.S., and Holt D.B., *Advances in Physics*, 13, 193, (1964).
25. Tetelman, A.S., *Acta Met.* 10, 813, (1962).
26. Fourier J.T., *Phil. Mag.* 10, 1027 (1964).
27. Mott N.F. "Dislocations and Mechanical Properties of Crystals" p. 458, Ed. Fisher J.C., Johnson, W.G., Thompson R., and Vreeland Jr. T., (Wiley, New York), (1957).
28. Grosskreutz J.C., *J. App. Phys.* 34, 372, (1963).
29. Grosskreutz J.C., and Waldow P., *Acta Met.* 11, 717, (1963).
30. Snowden K.U. *ibid* 11, 675, (1963).
31. Wilson R.N. and Forsyth P.J.E., *J. Inst. Met.* 87, 336, (1959-60).
32. Segall R.L. and Partridge P.G., *Phil. Mag.* 4, 912, (1959).
33. Segall R.L., Partridge P.G., and Hirsch P.B. *ibid* 6, 1493, (1961).
34. Waldron G.W.J., *Acta Met.* 13, 897 (1965).
35. Wei R.P. and Baker A.J., *Phil. Mag.* 11, 1087, (1965).
36. McGrath J.T. and Bratina W.J., *ibid*, 11, 429, (1965).
37. Segall R.L. "Electron Microscopy and Strength of Crystals" Ed. Washburn J. and Thomas J. p.515, (Interscience Publishers, New York), (1963).
38. Feltner C.E., *Acta Met.* 11, 817, (1963).
39. Grosskreutz J.C. and Shaw G.G., *Phil. Mag.* 10, 961, (1964).
40. Segall R.L. and Finney J.M., *Acta Met.* 11, 685, (1963).
41. Ham R.K., *Phil. Mag.* 7, 1177, (1962).

42. Mader S. and Thieringer H.M. Fifth Int. Conf. for Electron Microscopy (Philadelphia), J.3, (Academic Press, New York), (1962).
43. Valdre U. *ibid*, c.c. 15.
44. Hirsch P.B. "Relation between Structure and Strength in Metals and Alloys", p.40, N.P.L. Symposium No. 15, (Her Majesty's Stationery Office: London), (1963).
45. Seeger A. *ibid*, p.4.
46. Mader S. "Electron Microscopy and Strength of Crystals" Ed. Washburn J. and Thomas G., (Interscience, New York), (1963).
47. Ikem R.K. and Wright M.G., *Phil Mag.* 10, 937, (1964).
48. Valdre U. and Hirsch P.B., *ibid*, 8, 237, (1963).
49. Pelloux R.M.N. Boeing Scientific Research Laboratories Report D1-85-0304, (1963).
50. Hirsch P.B., Partridge P.G., and Segall R.L., *Phil. Mag.*, 4 721, (1959).
51. Swann P.R., *J. Inst. Met.* 91, 243, (1963).
52. Clark J. B. and McEvily A.J. Jr., *Acta Met.* 12, 1359, (1964).
53. Price R.J. and Kelly A. *ibid*, 11, 915, (1963). ~~106, (1963)~~
54. Broom T. and Ham R.K., *Proc. Roy. Soc.*, A242, 166 (1957).
55. Ham R.K. *Proc. Int. Conf. on Fatigue of Metals*, p.781, (London: Instn. Mech. Engrs.), (1957).
56. Johnson E.W. and Johnson H.H. *Trans. A.I.M.E.*, 233, 1333, (1965).
57. Rosenberg H.M. "Vacancies and Other Point Defects in Metals and Alloys" p.206, *Inst. Met. Monograph No. 23*, (1958).
58. Broom T., Molineux J.H., and Whittaker V.N., *J. Inst. Met.*, 94 357, (1955-56).
59. Adair A.M., Hook R.E., and Garrett H.J. *A.R.L.* 132, (1961) (Wright Air Development Centre, Aeronautical Research Laboratory Report. Wright Patterson A.F.B., Ohio).
60. Ruoff A.L. and Balluffi R.W. *App. Phys. Letters* 1, 59, (1962).
61. Portevin A. and le Chatelier F. *Comptes Rendus*, 176, 507, (1923).

62. Price R.J. and Kelly A., Acta Met. 12, 159, (1964).
63. Ardley G.W. and Cottrell A.H., Proc. Roy. Soc., A219, 328, (1953).
64. Boniszewski T. and Smith G.C., Acta Met. 11, 1965, (1963).
65. Marcinkowski M.J. and Lipsitt H.A., *ibid*, 10, 95, (1962).
66. Koch C.C. and Troiano A.R. Trans. Amer. Soc. Metals, 57, 519, (1964).
67. Edington J.W., Lindley T.C., and Smallman R.E., Acta Met. 12, 1025, (1964).
68. Edington J.W. and Smallman R.E., *ibid*, 12, 1313, (1964).
69. Bailey D.J., Flanagan W.F., and Miller G.E., *ibid*, 13, 436 (1965).
70. Balluffi R.W. and Ruoff A.L., U.S. Atomic Energy Commission Report T.I.D. 16369 10F2, (1962).
71. Handy B.B. J. Inst. Met. 83, 115, (1954-55).
72. Wilcox B.A. and Smith G.C., Acta Met. 12, 371, (1964).
73. Macheraugh E. and Vöhringer O. *ibid*, 11, 157, (1963).
74. Sperry P.R. *ibid*, 11, 152, (1963).
75. Phillips V.A., Swain A.J. and Eborall R., J. Inst. Met. 81, 625, (1952-53).
76. Paxton H.W. and Churchman A.T., Acta Met. 1, 473, (1953).
77. Kent K. G. and Kelly A., J. Inst. Met. 93, 536, (1964-65).
78. Krupnik N. and Ford H. *ibid*, 81, 601, (1952-53).
79. McReynolds A.W., Trans. Amer. Inst. Met. Eng. 185, 32, (1949).
80. Sylwestrowicz W. and Hall E.O. Proc. Phys. Soc. B64, 495, (1951).
81. Hall O.E., *ibid*, B64, 742, (1951).
82. Chadwick R. and Hooper W.H.L., J. Inst. Met. 80, 17, (1951-52).

83. Cottrell A.H. and Jawson M.A. Proc. Roy. Soc. A199, 104, (1949).
84. Cottrell A.H. "Dislocations and Plastic Flow in Crystals", (Oxford At The Clarendon Press: London), (1953).
85. Seitz F., Advanc. Phys. 1, 43, (1952).
86. Mott N.F., Phil. Mag. 43, 1151, (1952).
88. Mott N.F., *ibid*, 44, 742, (1953).
89. Kovács J., Nagy E., and Feltham P., *Ibid*, 9, 797, (1964).
90. Akulov H.S. *ibid*, 9, 767, (1964).
91. Kovács J. and Nagy E., Phys. Stat. Solidi 8, 795, (1965).
92. Saada G., Physica 27, 657, (1961).
93. Dawson, N.I., *ibid*, 31, 342, (1965).
94. Pistorius C.A. *ibid*, 27, 149, (1961).
95. Blewitt T.H., Coltman R.R., and Redman J.K. "Defects in Crystalline Solids", p.359, (London: The Physical Society), (1955).
96. Bolling G.R., Phil. Mag. 4, 537, (1959).
97. Peiffer H.R., J. App. Phys. 34, 298, (1963).
98. Harris S.G., "Vacancies and Other Point Defects in Metals and Alloys" p.220, Inst. Met. Monograph No. 23, (1958).
99. Russell B. and Vela P., Phil. Mag. 8, 677, (1963).
100. Russell B. private communication.
101. Hahn G.T. Acta Met. 10, 727, (1962).
102. Bailey J.E. and Hirsch P.B., Phil. Mag. 5, 485, (1960).
103. Bailey J.E. private communication with J.D. Livingston (104).
104. Livingston J.D., Acta Met. 10, 229, (1962).
105. Hordon M.J. *ibid*, 10, 999, (1962).

106. Lomer J.N. and Rosenberg H.M., *Phil. Mag.* 4, 467, (1959).
107. Levinstein H.J. and Robinson W.H., "Relation Between Structure and Strength" p.179, N.P.L. Symposium No. 15, (Her Majesty's Stationary Office: London), (1963).
108. Hull D., McIvor I.D., and Owen W.S., *ibid* p.595.
109. Haasen P. and Jesse J., *ibid*, p.137.
110. Johnson W.G. and Gilman J.J., *J. App. Phys.* 30, 129, 1959.
111. Gordon P., Dislocation counts on the copper specimens of P. Gordon are the results of J.E. Bailey given in a paper by L. M. Clarebrough, M.E. Hargreaves, and M.H. Loretto. The paper is published in the A.I.M.E. sponsored book "Recovery and Recrystallization of Metals", (Interscience, Wiley, N.Y.) (1962), Ed. L. Himmel.
112. Basinski Z.S., Dugdale J.D., and Howie A., *Phil. Mag.* 8, 1989, (1963).
113. Buck O., *Phys. Stat. Solidi* 2, 535, (1962).
114. Venables J. A., *Phil. Mag.* 7, 1969, (1962).
115. Basinski Z.S., Dugdale J.D., and Guban D., *ibid*, 4, 880, (1959).
116. Keh A.S. "Direct Observation of Imperfections in Crystals" p.213, (Interscience: New York), (1962).
117. Reid C.N., Gilbert A., and Rosenfield A.R., *Phil. Mag.* 12, 409, (1965).
118. Nakada Y. and Chalmers, B. *Acta Met.* 13, 925, (1965).
119. Hargreaves M.E., Loretto M.H., Clarebrough L.M., and Segall R.L., "Relation Between Structure and Strength" p.209, N.P.L. Symposium No. 15, (Her Majesty's Stationary Office: London), (1963).
120. Iyer A.S. and Gordon P., *Trans. Met. Soc. Amer. Inst. Min. (Metall.) Engrs.* 215, 729, (1959).
121. Ham R.K., private communication.
122. Halford G.R., Paper presented at the Fall Meeting of the Met. Soc. of A.I.M.E., (Detroit), October 1965.

123. Jaffrey D., Thesis, University of Queensland, 1963.
124. Abel, A., Thesis, McMaster University, 1965.
125. Basinski Z.S. private communication.
126. Ham R.K., Phil. Mag. 6, 1183, (1961).
127. Ruff A.W. Jr. and Kushner L.M., "Relation Between Structure and Strength in Metals and Alloys" p.145, N.P.L. Symposium No. 15, (Her Majesty's Stationery Office: London), (1963).
128. Girifalco L.A. and Grimes H.H., N.A.S.A. Tech. Report #R-38, (1959).
129. Miller G.E., Thesis, University of Washington, 1961.
130. Bailey D.J., Thesis, University of Washington, 1963.

Table I

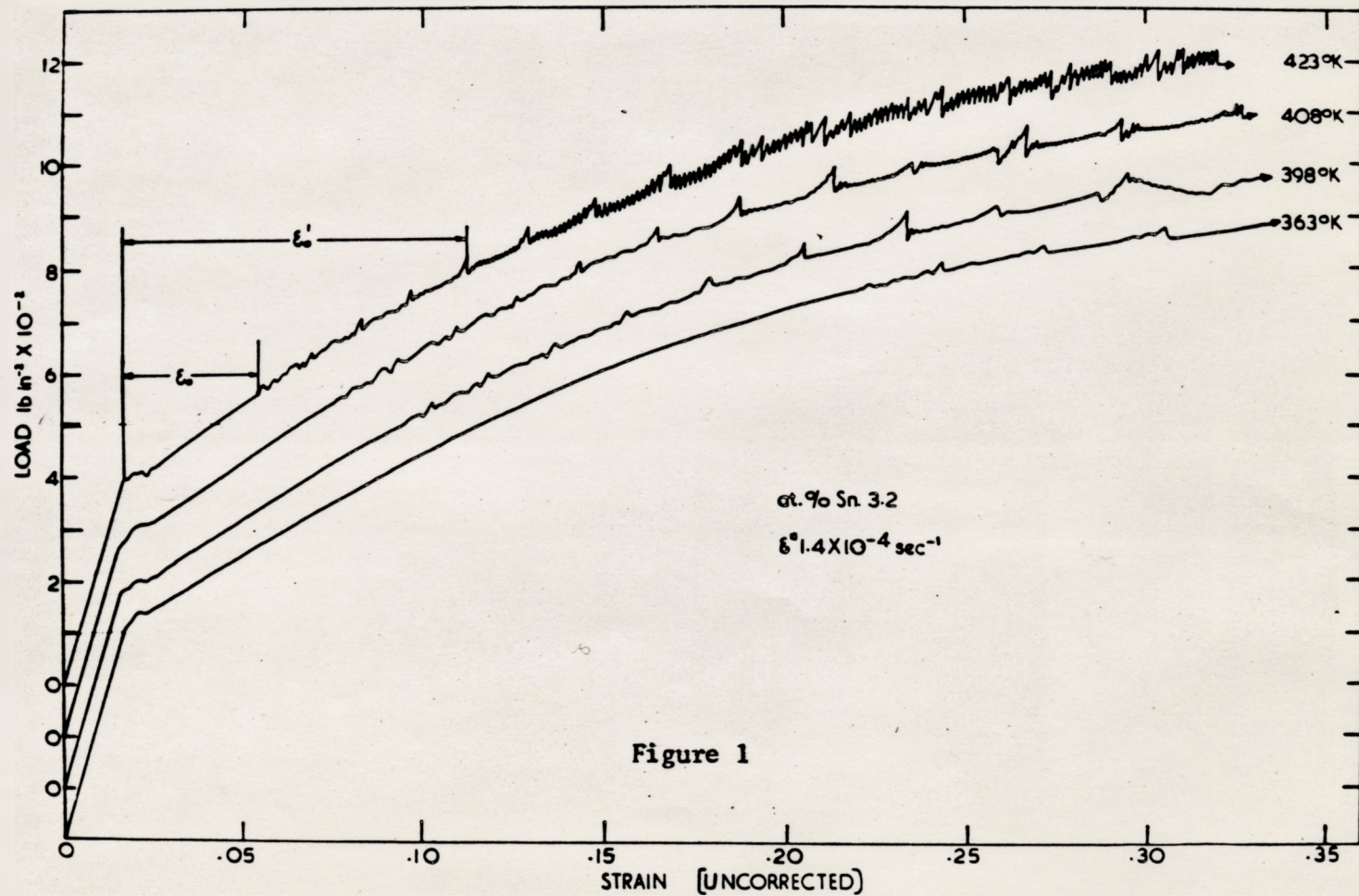
Metal	β	Reference
Ag	1.13	Bailey and Hirsch ⁽¹⁰²⁾
Cu	0.83	Bailey ^(103,104)
Cu-30%Zn	1.30	Lomer and Rosenberg ⁽¹⁰⁶⁾
V	0.68	Edington and Smallman ⁽⁶⁸⁾
Al	0.00	Waldron ⁽³⁴⁾
Al-0.5% Mg	0.30	Waldron ⁽³⁴⁾
Al-1.0% Mg	0.33	Waldron ⁽³⁴⁾
Al-3% Mg	0.61	Waldron ⁽³⁴⁾
Al-7% Mg	0.89	Waldron ⁽³⁴⁾

TABLE II

Foil or Spec. No	Temperature of Test °C	$\bar{\rho} \times 10^{-9} \text{ cm}^{-2}$	Standard error in $\bar{\rho}$	No. of determinations of ρ	Deformation History
8	25	3.39	0.24	53	1.61 \pm 0.1% tensile strain
3	25	5.37	0.40	46	2.29 \pm 0.4% tensile strain - 1.0
4	25	12.93	0.76	73	3.61 \pm 0.3% tensile strain
6	25	16.61	0.90	67	5.96 \pm 0.05% tensile strain
7	25	22.15	1.03	57	8.01 \pm 0.35% " "
23	140	9.56	0.64	30	3.812% tensile strain + 0.798% compressive strain
17	140	16.62	0.85	32	3.391% tensile strain + 4.977% compressive strain
22	140	19.43	1.25	52	3.391% tensile strain + 2.522% tensile strain

TABLE III

ϵ_{Pre}^b	ϵ_A^b	ϵ_{Tot}^b	$\epsilon_{Tot}^{1.17}$	$\epsilon_{Tot}^{2.2}$	$\epsilon_{Pre}^{1.03}$	$\epsilon_{Tot}^{2.2} - (\epsilon_{Tot}^{1.17} \cdot \epsilon_{Pre}^{1.03})$
0	4.667	4.667	-	29.51	-	29.51
0.689	4.365	5.054	6.639	35.33	0.681	30.81
1.013	4.123	5.136	6.767	36.53	1.0156	29.68
1.023	4.290	5.313	7.050	39.41	1.0259	32.17
3.100	3.160	6.260	8.542	56.56	3.2070	29.16
3.391	1.974 (Ten)					
3.391	4.134 (Com)					



Typical load-extension curves obtained by straining a 3.2 at. % Sn alloy at a strain rate of $1.4 \times 10^{-4} \text{ sec}^{-1}$ at the temperatures indicated. No correction has been made to allow for machine elasticity.

FIG. 2. Electrical resistivity as a function of elongation strain for a representative specimen. The ----- extensions of the curves represent continuations of the data if no recovery anneal is performed. The discontinuities marked with ----- lines arise at the strains where a room temperature recovery is performed. The resistivities ρ_0' increase as the strain increases. The recoverable resistivity is approximately 30% of the total resistivity increase introduced above the fully annealed resistivity ρ_0 .

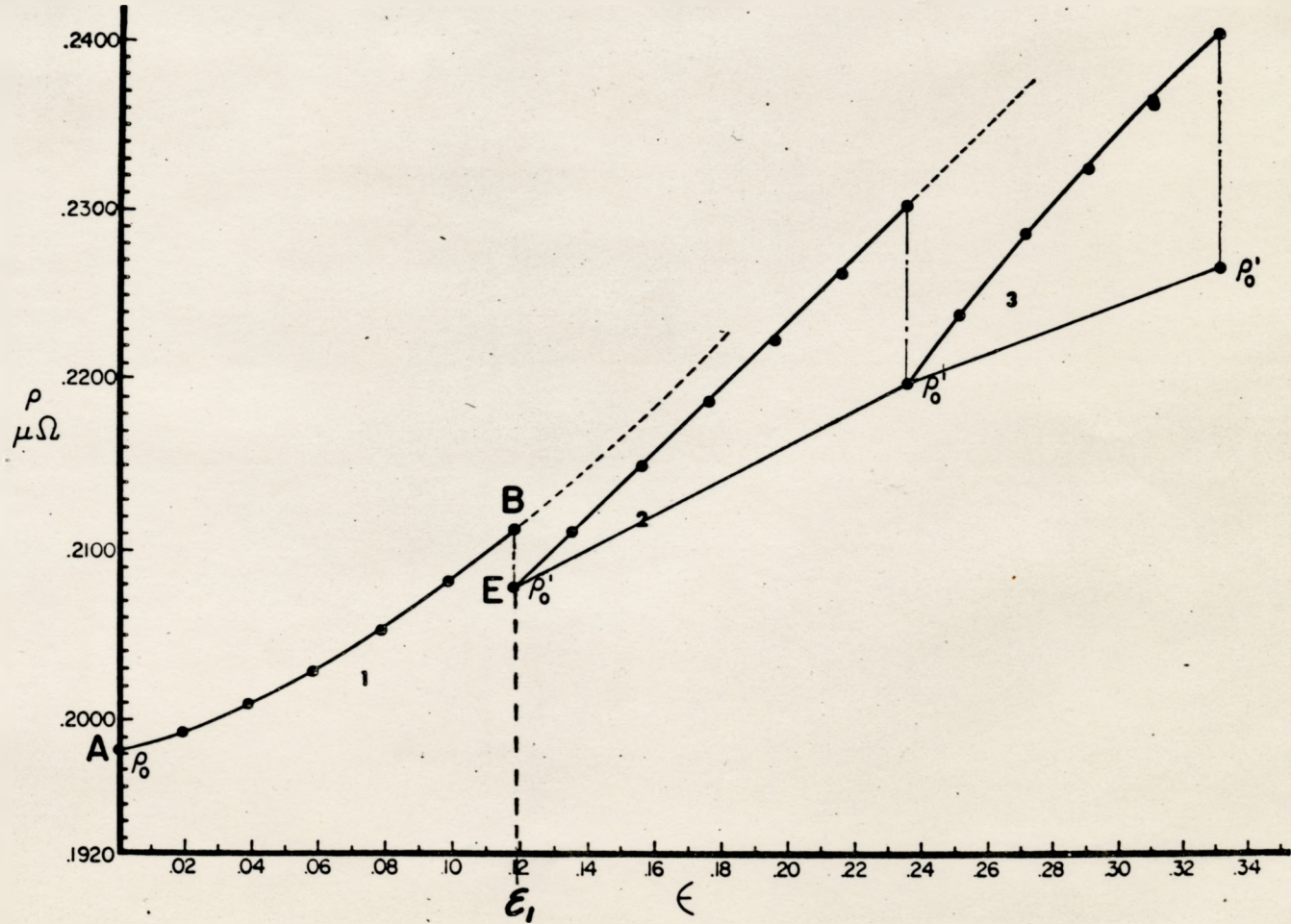


Figure 2
Peiffer's Results

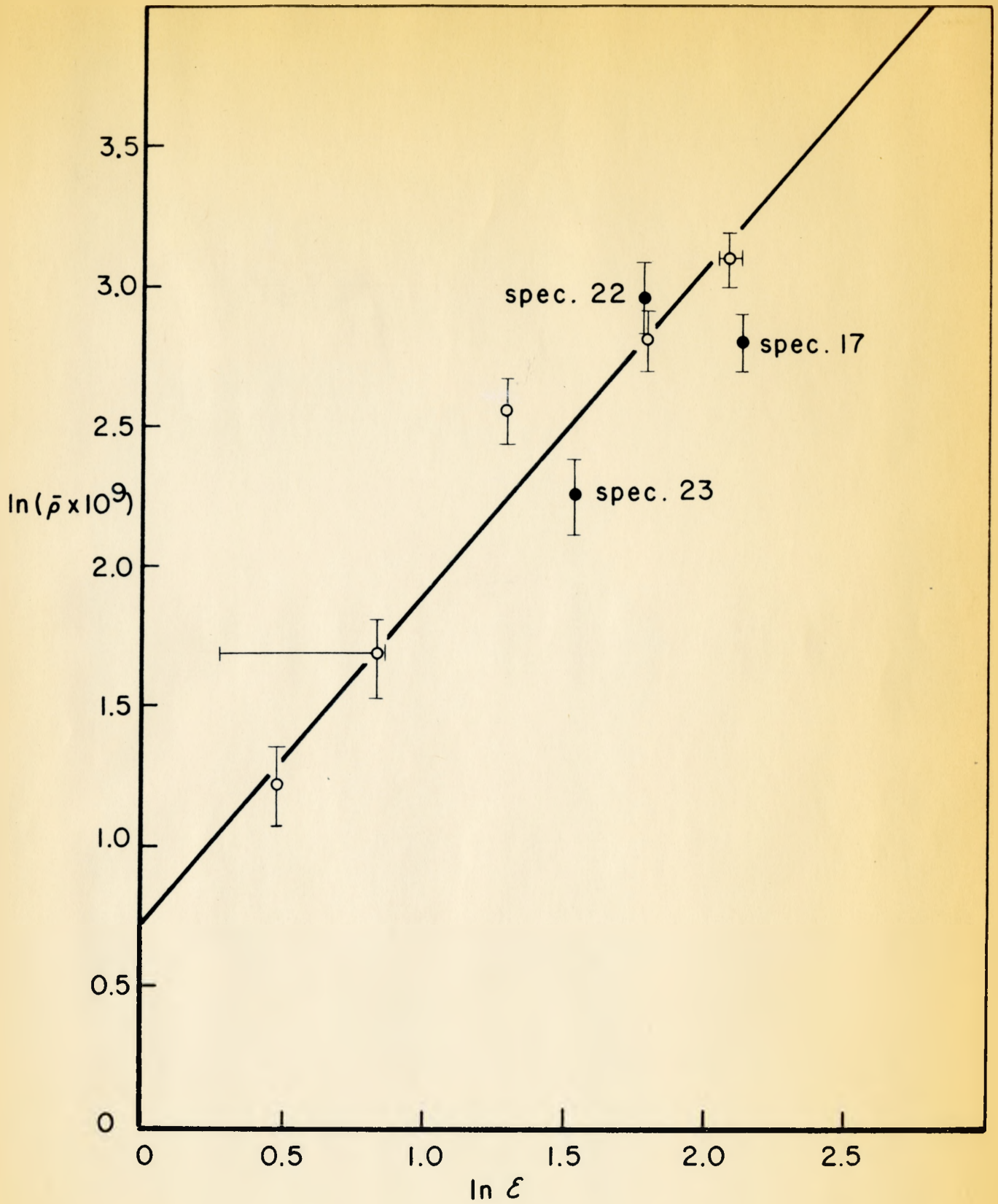


Figure 3
 log Mean Dislocation Density
 vs
 log Total True Plastic Strain

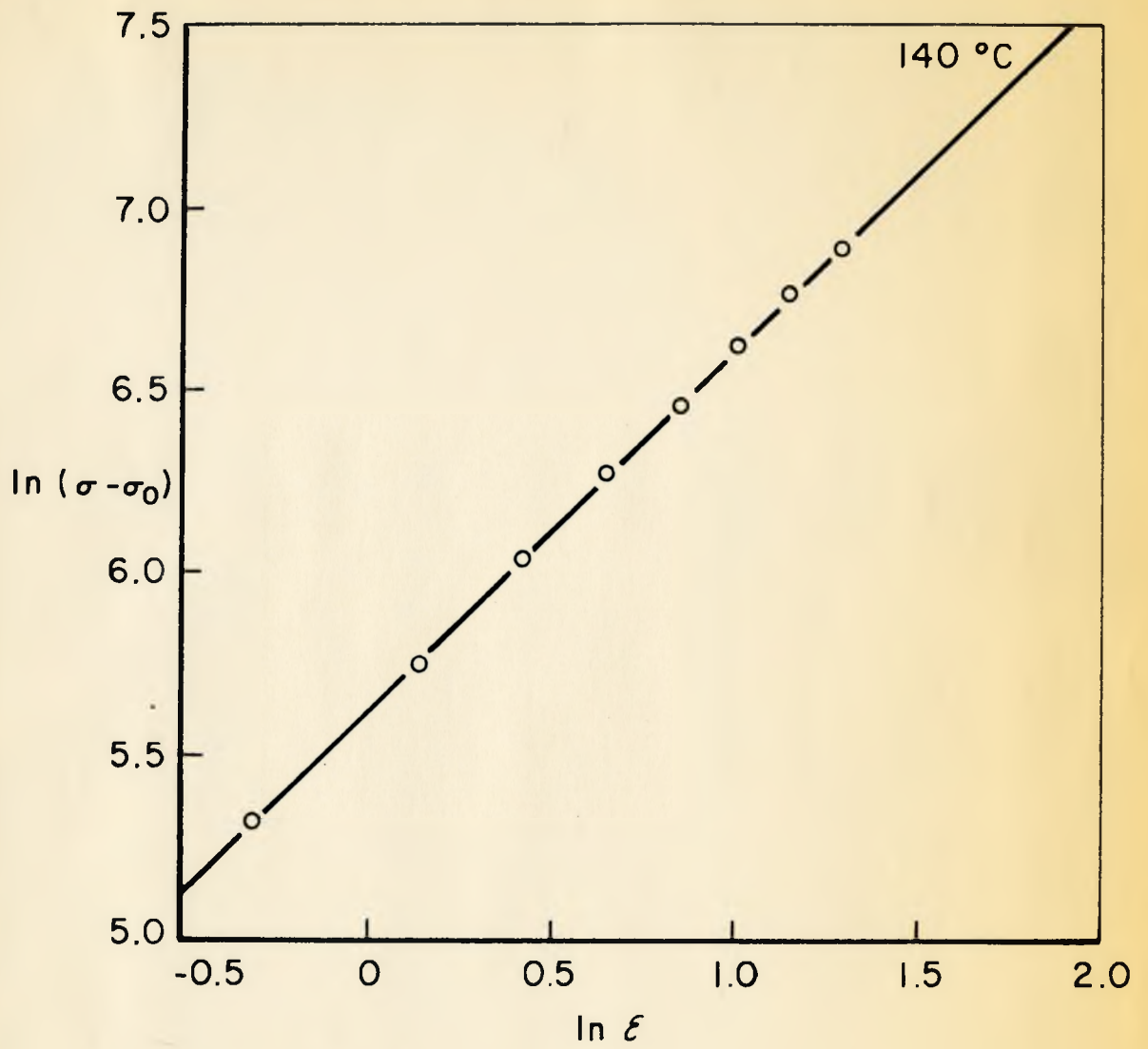


Figure 4
log flow stress increment
vs
log true plastic strain

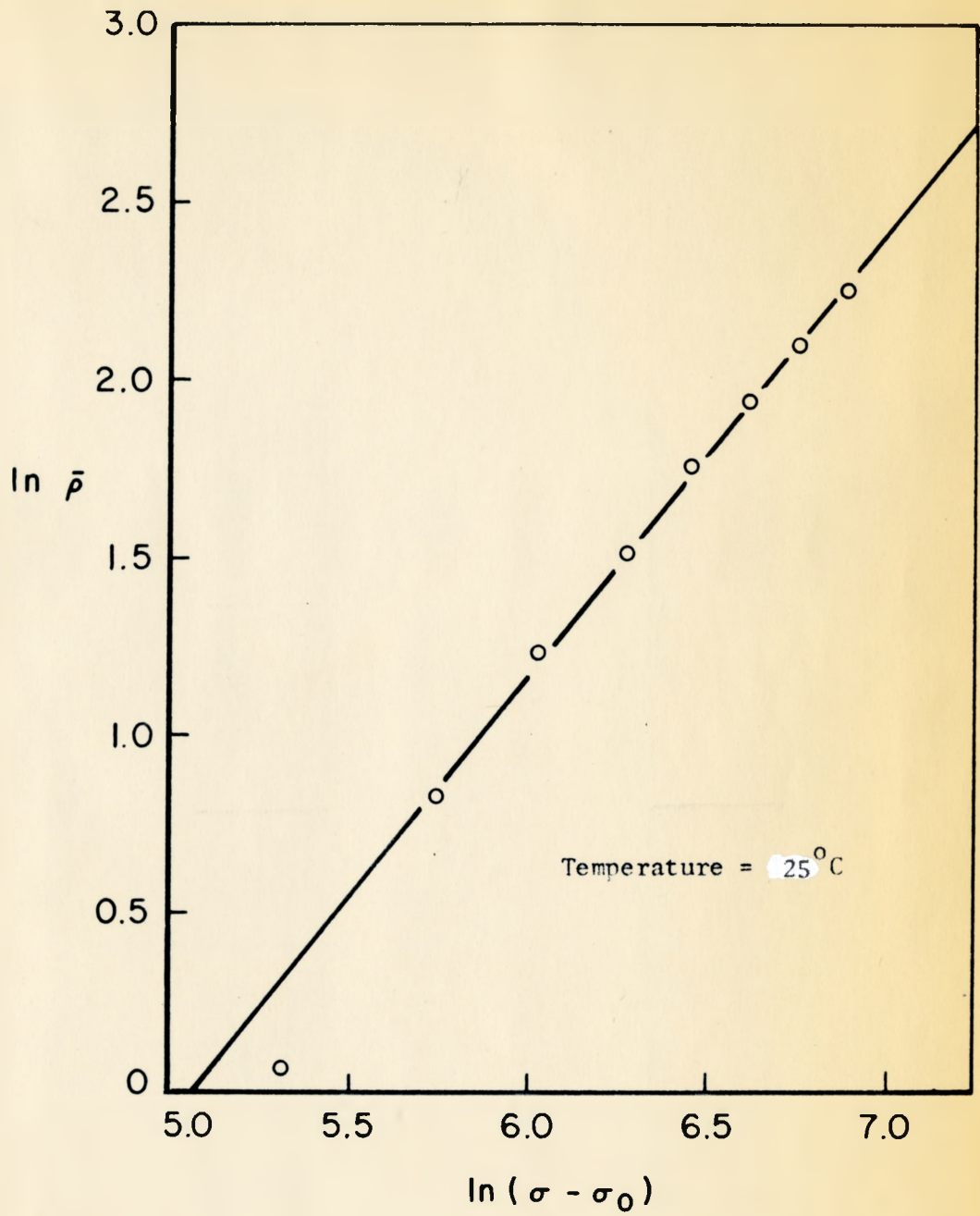


Figure 5

log mean dislocation density
vs
log flow stress increment

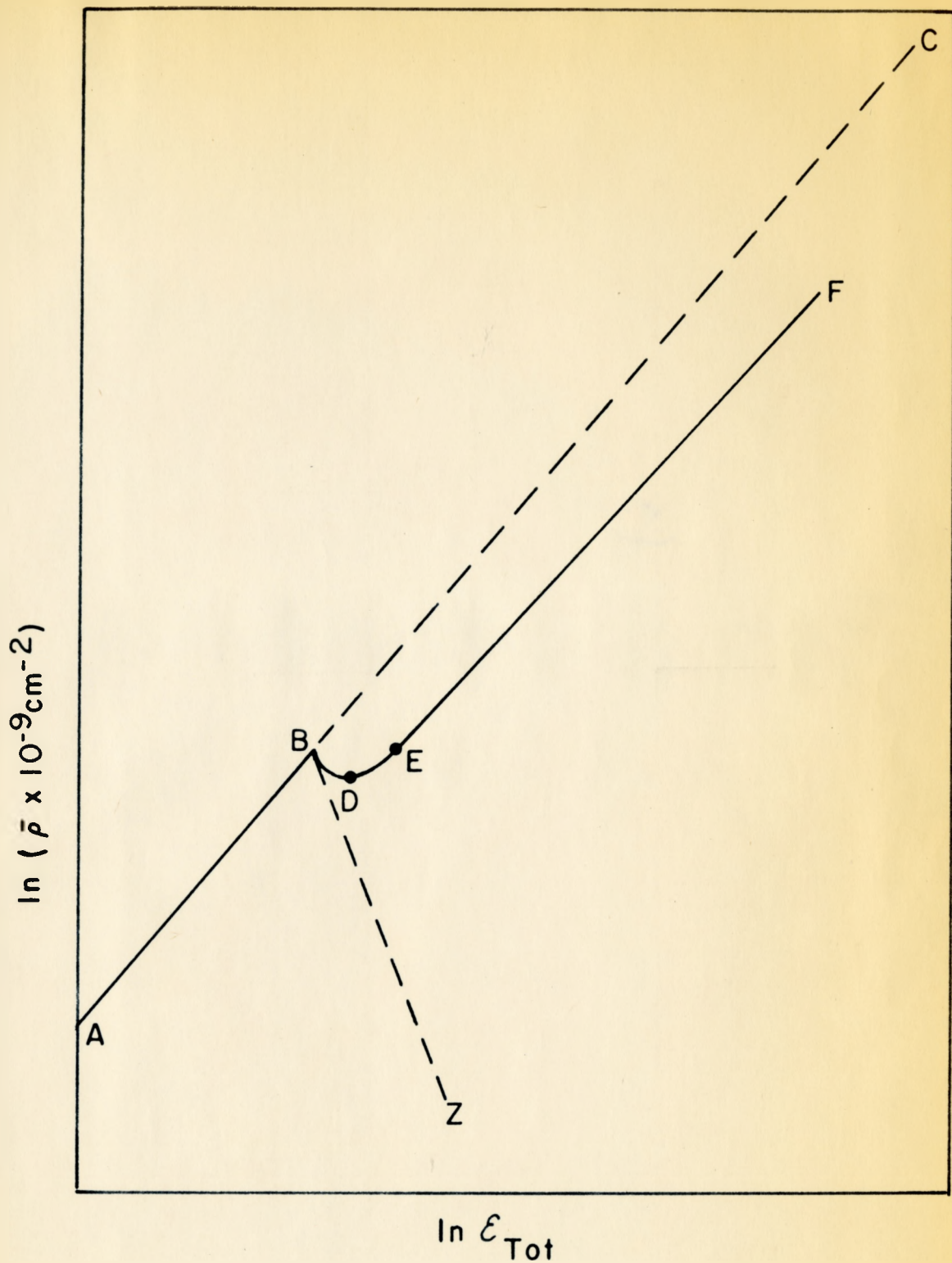


Figure 6

Hypothetical plot of $\log \bar{\rho}$ vs ϵ_{Tot} for tensile pre-strain followed by compressive strain.

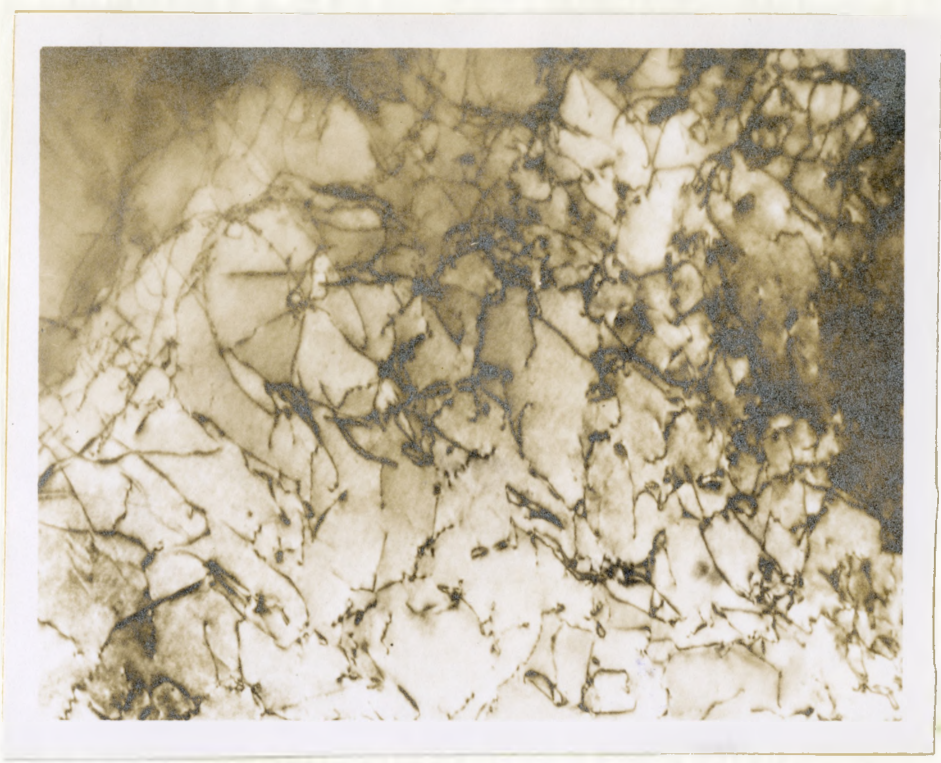


Figure 7: Typical Microstructure of specimen 22. Magnification 58,250 X.

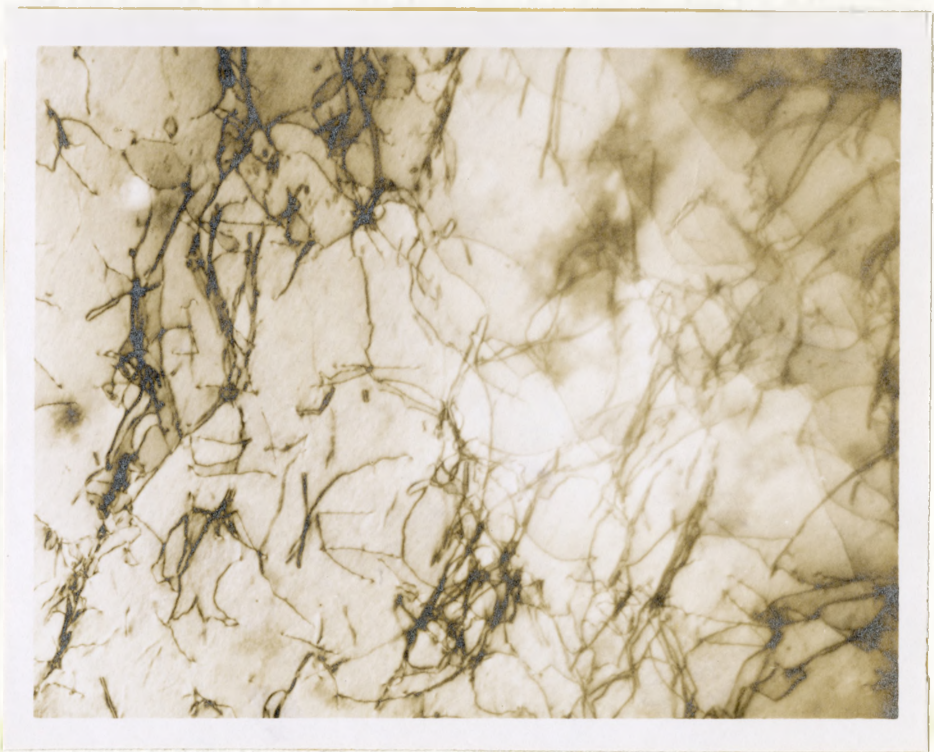


Figure 8: Typical microstructure of specimen 17. Magnification 31,000 X.